INSTITUTE OF SOLID STATE PHYSICS
BULGARIAN ACADEMY OF SCIENCES

EVGENY KONSTANTINOV POPOV

ANOMALIES IN RELIEF DIFFRACTION GRATINGS

SUMMARY

of a thesis for awarding a Doctor of Sciences degree

Sofia, 1990

ОТПЕЧАТАНО В ПЕЧАТНАТА БАЗА
НА С Н Р Б
БУЛ."ЛЕНИН" № 73
СОФИЯ,1990

Devoted to the memory of
my friend and teacher
Lyuben Mashev

INTRODUCTION

Contrary to common sense, scientist is usually thrilled with the word 'anomaly'. This paradox could easily be explained - anomaly means something abnormal, unexpected, i.e. unpredicted, novel. When R.Wood in 1902 observed some unexpected property of diffraction gratings - diffraction efficiency changes more than 10 times in the spectral region not larger than the distance between sodium lines, he called that phenomenon 'anomalous'. This term proves to be so fascinating that even when some anomalies find their explanation (become 'normal' from a theoretical point of view) phenomena they represent continue to be called anomalous.

Explained or not, each more or less rapid change in diffraction efficiency of gratings is called anomaly. Great interest in almost century lasting investigation of anomalies could find its explanation in the following reasons:

1. Their appearance is connected with some physical phenomena that attract attention by themselves.
2. Many of the anomalies are connected with surface wave excitation and could provide information for their properties.
3. For the most of grating applications it is more important to have smooth, rather than very high diffraction efficiency - anomalies must be avoided.
4. It appears that in some cases very high efficiency values could be anomalous, too. Detailed investigations of anomalies could result in some interesting applications.
5. Theory of anomalies provides incomparable stimuli for development of recent numerical methods for analysis of light diffraction by relief gratings.

The necessity of the thesis is due mainly to the lack of detailed investigation of <u>all</u> anomalies. In the last years new anomalies have been discovered that make it possible to develop a new united classification of anomalies and to determine the connections that exist between them. The <u>aims</u> of the investigation when working on

the thesis were:

1. Developing program packages based on the recently published or original rigorous methods for analysis of light diffraction by relief gratings, verification of the computer codes and determination of their efficiency and regions of application.

2. Theoretical and experimental investigation of some anomalies in different types of gratings (metallic, dielectric and multilayered) and of the possibility of utilizing anomalous properties.

3. Determination of physical connections between different anomalies and reasons for their appearance. This was done on two levels:

a) phenomenological - it enabled to draw connections between anomalies;

b) microscopical - what are the properties of electromagnetic field in the near zone of diffraction and how its peculiarities influence the far-field diffraction efficiency.

The thesis consists of 10 chapters divided in three parts. The first part contains three chapters. It deals with the general features of light diffraction by relief gratings (statement of the problem, some main theorems), historical review of investigations on anomalies and their recent classification. Chapter three contains a review of the theoretical methods, including a detailed presentation of the used in our laboratory rigorous numerical method.

Part two presents anomalies in bare metallic gratings - resonance (chapter 5) and non-resonance (chapter 4 and 6) and some examples of their interaction (chapter 7). It is shown how some general properties of metallic gratings could be explained from a microscopical point of view.

Part three analyzes anomalies in corrugated dielectric waveguides - what is the influence of waveguide mode excitation on the diffraction efficiency without (chapter 8) and with (chapter 10) mode interactions. Anomaly in the coefficients of mode coupling (planar Brewster's effect) is studied in chapter 10. Non-resonance anomalies in bare dielectric gratings are discusses in chapter 9.

PART ONE: LIGHT DIFFRACTION BY RELIEF GRATINGS

CHAPTER ONE: BASIC PROPERTIES OF DIFFRACTION GRATINGS

Statement of the problem of light diffraction by relief diffraction grating shown schematically in fig.1.1 is presented in §1. Main properties of gratings are discussed including grating equation, reciprocity theorem, invariance theorem. §2 contains a brief review of common properties and peculiarities the spectral dependencies of metallic gratings having different profiles and groove depths.

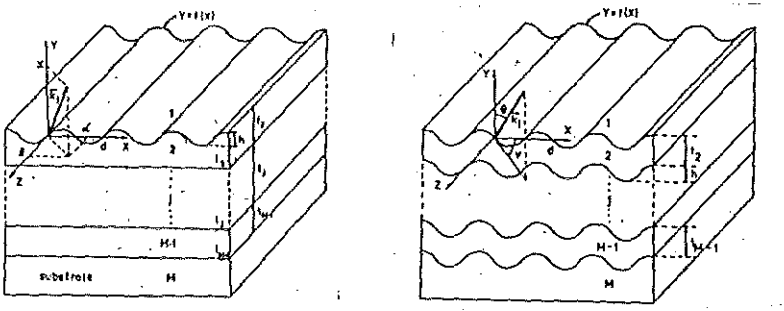

a b

Fig.1.1. Schematical representation of relief diffraction grating.

Historical review on grating anomalies is presented in §3. Recent classification of different types of anomalies is given in §4:

I. Resonance anomalies which are accompanied by sharp electromagnetic field enhancement in the near vicinity of grating surface. They are due to guided wave excitation along the corrugated surfaces.

II. Non-resonance anomalies that can be divided in two types:

1. Anomalies in Littrow mount - angular and spectral dependence of efficiency is smoother than in the region of resonance anomalies. Littrow mount (sometimes called Bragg-type) anomalies are not connected with surface wave excitation but with some peculiarities in energy flow distribution - formation of curls inside deep grooves. Usually these anomalies do not lead to any noticeable drop in the total reflected light.

2. Non-resonance anomalies that are in connection with the existence of guided waves but in the interval of parameters where such waves are

forbidden (chapter 5 and 6).

Of course with a suitable choice of conditions it is possible to have a simultaneous appearance of two or more anomalies, their interaction and even 'annihilation'.

It is important to note that one and the same phenomenon could result in different anomalies in different diffraction orders. That is why anomalies in the 0th and -1st orders are considered separately in the corresponding chapters.

CHAPTER TWO: SURFACE WAVES AND RESONANCE ANOMALIES

This chapter explains the mechanism by which surface wave excitation leads to anomalies in the diffraction efficiency. For this aim a brief review is presented of surface waves that propagate along plane metal-dielectric boundary and in multilayered planar waveguides. § 2 contains the so called phenomenological approach that represents surface wave excitation in corrugated system by a set of zeros α^z and poles α^p of the scattering matrix S [19, 20]. Its components could be represented in the resonance anomaly region by the phenomenological formula:

$$S_{ij} = \frac{\alpha_0 - \alpha^z_{ij}(h)}{\alpha_0 - \alpha^p(h)} \quad , \qquad (2.1)$$

where α_0 is the sinus of angle of incidence. Without corrugation $\alpha^z \equiv \alpha^p$ and there are no anomalies. Existence of grating leads to the splitting of pole and zeros. Tracing of their trajectories in the complex α_0 plane as a function of groove depth and/or wavelength is a strong tool for investigation of anomaly connections and origin.

When incident wave vector is not perpendicular to the grooves (conical diffraction mounting), representation (2.1) becomes more complicated. Using reciprocity theorem it is shown how arbitrary polarized incident wave can be decomposed into two mutually orthogonal components (in general, elliptically polarized). One of them (with amplitude p_i) is not interacting with the surface wave. Thus in the phenomenological formulae (2.1) a new slowly varying term is added, proportional to p_i.

§ 3 discusses the two main features of mode interaction: 1) its influence on the resonance anomalies and how it can be reflected in the phenomenological formulae; 2) energy transfer between interacting modes, variation of their amplitudes in the corrugated region and mode

coupling equations. A generalization of the phenomenological approach is proposed that makes it possible any numerical treatment for light diffraction of plane waves on grating to be utilized for determining the coupling coefficients when two modes interact in the corrugated region of a planar waveguide, as follows:

Solution of eigenproblem means that the determinant of the matrix inverse to the scattering one has a zero - $\det(S^{-1})=0$. This means that the rank of S^{-1} is smaller than its order, i.e. a linear connection exists between its columns and, in particular, between j-th diffracted order amplitude (b_ν) and the resonance amplitude b_μ. Varying grating period it is possible to have a second resonance and in the linear connection $b_\nu = c_{\nu\mu} b_\mu$ a pole K_ν^p appears:

$$b_\nu = \frac{c_{\nu\mu}}{K - K_\nu^p}\, b_\mu \quad . \tag{2.2}$$

Let us suppose that the grating region is extended from x=0 to x=L, where L>>d. The μ-th mode amplitude can be represented in Fourier series:

$$b_\mu(x) = \frac{1}{2\pi} \int_{-\infty}^{\infty} B_\mu(K)\, e^{iKx}\, dK \quad , \tag{2.3}$$

where $B_{\mu,\nu}(K)$ are the Fourier components corresponding to a fixed grating vector K. Using (2.2) the response to the set of amplitudes $\{B_\mu(K)\}$ is:

$$b_\mu(x) = \frac{1}{2\pi} \int_{-\infty}^{\infty} B_\nu(K)\, \frac{c_{\mu\nu}}{K - K_\mu^p}\, e^{iKx}\, dK \quad . \tag{2.4}$$

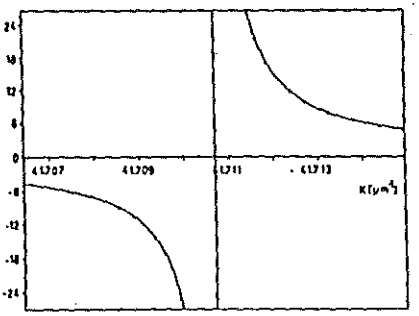

ig.2.1. Ratio b_1/b_0, calculated y the rigorous metod (solid line) nd using eq.(2.2) (represented ith crosses with c_{01}=0.0201 μm^{-1}, '=41.7107 μm^{-1}) as a function of for a waveguide with n_1=1, =2.3, n_3=1.6, t=0.3 μm, h=0.004 , λ=0.6 μm and angle of incidence φ=30°.

After differentiation of (2.4) in x the following equation is deduced:

$$\frac{d}{dx} b_\mu(x) = i\frac{c_{\mu\nu}}{2\pi} \int_{-\infty}^{\infty} B_\nu(K) \frac{K}{K_\mu - K^p} e^{iKx} dK = iK_\mu^p b_\mu(x) + c_{\mu\nu} b_\nu(x) \quad (2.5)$$

where we have assumed that $c_{\mu\nu}$~const. This statement needs more precise analysis. In fig.2.1 a comparison between the numerically calculated ratio b_ν/b_μ and that obtained from (2.2) is presented and a very good agreement is achieved for a large region of K, except for the near vicinity of pole interaction point where $\mathrm{Im}(\alpha^p)$ becomes large enough that the equation $\det S^{-1}$ is no longer fulfilled for real values of α_0.

Introducing another set of slowly varying amplitudes $\tilde{b}_\mu = b_\mu \exp(-iK_\mu^p x)$ in (2.5), the well-known system of coupled mode equations is obtained:

$$\begin{aligned} \frac{d\tilde{b}_\mu(x)}{dx} &= i\, c_{\mu\nu}\, \tilde{b}_\nu(x)\, e^{i\delta_{\mu\nu}x} \\ \frac{d\tilde{b}_\nu(x)}{dx} &= i\, c_{\nu\mu}\, \tilde{b}_\mu(x)\, e^{-i\delta_{\mu\nu}x} \end{aligned} \quad (2.6)$$

where $\delta_{\mu\nu} = K_\mu^p - K_\nu^p$ is the deviation from the Bragg condition.

CHAPTER THREE: THEORETICAL METHODS FOR ANALYSIS OF LIGHT DIFFRACTION BY RELIEF GRATINGS

A brief review of different theoretical methods - approximate and rigorous, for analysis of plane wave diffraction by relief grating is presented in §1. It includes different approximate methods based on the Rayleigh hypothesis, rigorous integral and differential methods.

§2 contains a detailed presentation of an original differential method – a generalization of the rigorous differential formalism of Chandezon et al. (C-method) in two directions: for conical mounting and for gratings with a corrugation only on the upper boundary (fig.1.1a). The choice of the method has been determined by its wide field of application (metal, dielectric and multicoated very deep gratings). On the other hand this method does not need so complicated mathematics and is not so time consuming. The transformation of the coordinate system:

$$\left| \begin{array}{l} u = x \\ v = y - f(x) \\ w = z \end{array} \right. \quad (3.1)$$

transforms the Maxwell's equations in each of the layers of fig.1b

into a system of 4 partial differential equations with non-constant coefficients:

$$\frac{\partial E_v}{\partial v} = \mathcal{D}(u)\frac{\partial E_v}{\partial u} + i\omega\mu_0\mathcal{E}(u)\left[H + \frac{1}{k^2n^2}\frac{\partial}{\partial w}\left[\frac{\partial H_u}{\partial w} - \frac{\partial H_v}{\partial u}\right]\right] , \qquad (3.2a)$$

$$\omega\mu_0\frac{\partial H_u}{\partial v} = \omega\mu_0\frac{\partial}{\partial u}\left[\mathcal{D}(u)H_u\right] + ik^2n^2E_v - i\frac{\partial}{\partial u}\left[\mathcal{E}(u)\left[\frac{\partial E_u}{\partial w} - \frac{\partial E_v}{\partial u}\right]\right] , \qquad (3.2b)$$

$$\omega\mu_0\frac{\partial H_v}{\partial v} = \omega\mu_0\mathcal{D}(u)\frac{\partial H_v}{\partial u} - i\mathcal{E}(u)\left[k^2n^2E_u + \frac{\partial}{\partial w}\left[\frac{\partial E_u}{\partial w} - \frac{\partial E_v}{\partial u}\right]\right] , \qquad (3.2c)$$

$$\frac{\partial E_u}{\partial v} = \frac{\partial}{\partial u}\left[\mathcal{D}(u)E_u\right] - i\omega\mu_0H_v + \frac{i\omega\mu_0}{k^2n^2}\frac{\partial}{\partial u}\left[\mathcal{E}(u)\left[\frac{\partial H_u}{\partial w} - \frac{\partial H_v}{\partial u}\right]\right] , \qquad (3.2d)$$

where μ_0 is the vacuum permeability, k is the wave number, n - the refractive index and $\mathcal{E}(x)=[1+f'(x)^2]^{-1}$, $\mathcal{D}(x)=f'(x)\mathcal{E}(x)$. Unlike the classical diffraction case ($\beta_0=0$) the system (3.2) and the unknown field components cannot be split up into two independent sets, corresponding to the two fundamental polarizations.Taking into account the periodicity of the grating, the solution of (3.2) can be sought in the form:

$$F = \begin{bmatrix} F^1 \\ F^2 \\ F^3 \\ F^4 \end{bmatrix} = \begin{bmatrix} E_v \\ \omega\mu_0 H_u \\ -\omega\mu_0 H_v \\ E_u \end{bmatrix} , \qquad (3.3)$$

where

$$F^p(u,v,w) = \sum_{m=-\infty}^{\infty} F^p_m(v)\, e^{ik(\alpha_m u+\beta_0 w)} , \quad p=1,\ldots 4 . \qquad (3.4)$$

and $\alpha_m=\alpha_0+\lambda/d$. For a numerical treatment a limited number $m\in[-N,N]$ of orders has to be taken into account. If G stands for the truncated vector F (3.2) can be written in a matrix form:

$$-i\frac{dG_j}{dv} = R^j G_j , \qquad (3.5)$$

where the components of R^j are obtained substituting (2) into (1). The solution of (3.5) can be represented by:

$$G_j = T^j_C \Phi^j(v) B^j , \qquad (3.6)$$

where

$$\Phi^j_{mp}(v) = \delta_{mp}\exp(ir^j_m v) . \qquad (3.7)$$

is a square (8N+4)x(8N+4) matrix with columns - the eigenvectors of

R^j, r^j are the corresponding eigenvalues and B^j contains the unknown amplitudes determined by the boundary and outgoing wave conditions. In the Ouvw coordinate system the boundaries between the layers are defined by $v=l_j$ and a connection between the unknown amplitudes at the two sides of the j-th boundary is quite simple:

$$T_c^j \Phi^j(l_j) B^j = T_c^{j+1} \Phi^{j+1}(l_j) B^{j+1}. \qquad (3.8)$$

Using (3.8) a connection between the amplitudes in the upper and lower media can be found. Taking into account the outgoing wave conditions the system (3.2) is reduced to a more simple linear algebraic system.

The description of the system shown schematically in fig.1.1a needs a complication of field representation in the second region. For $y<\min[f(x)]$ the field can be expanded in plane waves:

$$\tilde{F}^j = Q V_j \tilde{\Phi}^j(y) \tilde{B}^j e^{ik\beta_0 z}, \qquad (3.9)$$

where $Q_{mp}=\delta_{mp}\exp(i\alpha_m x)$ and $\tilde{\Phi}^j_{mp}(y)=\delta_{mp}\exp(i\chi^j_m y)$, $\chi^2_m=n^2-\alpha^2_m$. The uniqueness of the solution in the second region connects $\tilde{F}^2\big|_{y=l_2}$ and B^2. The boundary conditions at the flat boundaries $y=l_2,\ldots l_{m-1}$ make it possible to express the diffracted waves amplitudes via the incident ones.

It has been pointed out that the most important criterion of the quality of a numerical method is its efficiency - ability to deal with a wide class of gratings in a relatively short computation time, rather than its simplicity. It is well known that the computation time in the matrix operations is proportional to the cube of the matrix size, so the most important factor becomes the convergence rate with respect to the truncation parameter N. We have made a set of calculations in order to perform the limits of method applications for

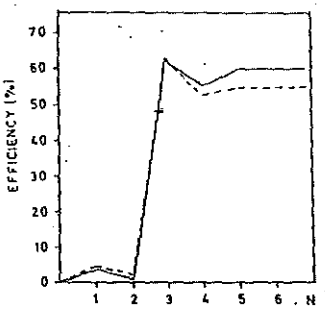

Fig.3.1. Convegence rate for $\varphi'=0°$ (solid line) and $\varphi'=60°$ (dashed line). Grating period is equal to the depth - 0.6 μm. For $\varphi'=30°$ the results coinside with the case $\varphi'=0°$. In the in-plane case $\lambda=0.6$ μm.

fferent types of gratings. It happens that the saturation value is tained at one and the same N independent of the angle φ between the cident wave vector and the plane perpendicular to the grooves rresponding to the deviation from the classical diffraction case. As example in fig.3.1 the -1st diffraction order efficiency of a bare nusoidal Al grating is shown for three different values of φ: 0°, ° and 60° for a TM polarized incident light; the convergence is one d the same for the three cases. That is why in the next examples ly the classical diffraction case is investigated and the nclusions are valid for the Chandezon's formulation, too. A mparison has been made with the well- known Rayleigh-Fourier (RF) n-rigorous method and for metal, dielectric and coated gratings the llowing general conclusions can be drawn:

The results of Wirgin [67, 68] concerning the validity of the RF thod for sinusoidal gratings with depth far exceeding the eoretical limit are confirmed. On the other hand the rigorous method oth in the conical and classical cases) has a faster convergence ich diminishes much slower than that of the RF method - for gratings moderate and high depth values (h/d>0.2) the computer time gain mpensates the sophistication of the code. In fig.3.2 the convergence tes of the two methods are compared for an Al grating - for small N e results of the RF method are highly oscillating while the rigorous thod converges much faster.

The change of the grating profile worsens drastically the vergence of the RF method, not affecting significantly the iciency of the rigorous method (fig.3.3).

Even for shallow gratings, above some critical thickness of the :ing t_{max}, different for the two methods, the results diverge. This iculty was reported by Chandezon et al. [95], but without any anation. Moreover, increasing N the critical thicknesses decrease, results being worse for the RF method. For example, when h/d=0.43 igorous method is applicable to four times greater values of the e layer thickness. We have found that this divergence is due to finite computer word length: For the propagating diffraction s the modulus of the exponential propagation factors is equal to The evanescent waves are characterized by complex propagation s and if their real exponents are large enough, in the matrix lications the small members are truncated. For the 32 bits

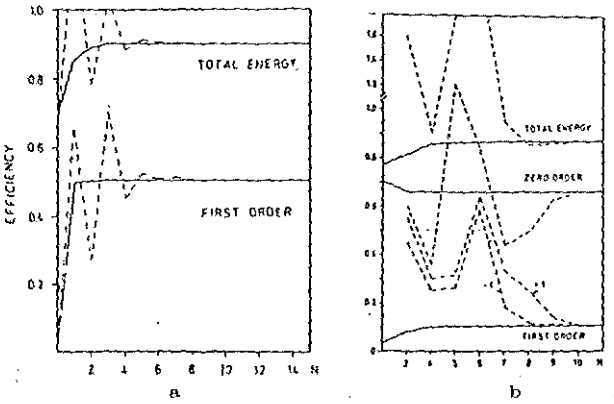

Fig.3.2 Convergence rate for RF (dased line) and for rigorous method (solid line) - sinusoidal Al grating
(a) h/d=0.333
(b) h/d=0.6 . .

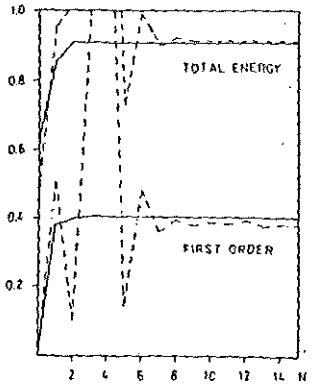

Fig.3.3. Like fig.3.2a, exept for a symmetrical triangular profile.

computer word length 23 bits are reserved for the mantissa and if

$$\max_m |\mathrm{Im}(\chi_m)| = H_N^I$$
$$\max_m |\mathrm{Im}(r_m)/k| = H_N^{II} \quad , \quad -N \le m \le N \quad , \qquad (3.10)$$

the maximum available thickness t_{max} can be given as $2\pi t_{max} H_N/\lambda < \ln(2^{23})$. The values of t_{max} for the RF (0.27μm) and for the rigorous method (0.56μm) obtained from this inequality are close to the numerically calculated 0.23μm and 0.47μm, respectively, wher

h/d=0.34, for example.

§3 contains a short classification of different theoretical methods for analysis of mode coupling in corrugated waveguides. Approximate analytical methods, usually valid in first order approximation with respect to the modulation depth are considered in the beginning. First attempts consist of substituting the perturbation of boundaries with a perturbation of Maxwell's equations. Their solution is searched as a sum of modes of the unperturbed waveguide (ideal mode approach) or of the planar waveguide with thickness corresponding to the local thickness (local mode approach). The periodicity of the corrugation leads to the coupled mode equations. Unfortunately, these approaches are valid only for collinear coupling because of not taking into account the exact boundary conditions. At the other hand, the existence of such analytical method that could give the mode coupling coefficients in closed form is important in Integrated optics. In great amount of integrated optical devices the corrugation depth is much smaller than the period and the waveguide thickness in order not to modify significantly mode field distribution and propagation constant. In that case it is quite useful to obtain some formulas, although being approximate, but enabling the calculation of the coupling coefficients without heavy computer codes and big computers.

As a first step mode coupling by a single step structure on a waveguide with an arbitrary refractive index profile is considered. On both sides of the step the field is represented as a superposition of all possible modes (guided and radiated) of a waveguide with a suitable thickness, propagating in all possible directions. The mode amplitudes are evaluated using the boundary conditions on the step boundary. In a first order approximation in step height analytical expressions are obtained and, in particular, the dependence of the TE_{μ}-reflected mode amplitude on the amplitude of the TE_{η}-incident one takes the form:

$$a_{\mu}^{I-} = a_{\eta}^{I+} \cdot h \frac{s_{\mu\eta}}{2} \left\{ \frac{\gamma_{TE\eta}}{\gamma_{TE\mu}} - \left| \frac{\cos\psi_{TE\eta}}{\cos\psi_{TE\mu}} \right| \right\} , \qquad (3.11)$$

where $s_{\mu\eta}$ is a coefficient depending on the waveguide parameters.

A groove with an arbitrary profile is divided into rectangular slides with infinitesimal width. Applying consecutively the boundary

conditions on each of the slide boundaries, the changes of the mode amplitudes are in a first order approximation in groove height proportional to:

$$i\,\Delta_{\mu\eta}\int_{\Lambda_0}^{\Lambda_0+\Lambda} f(x)\; e^{i\Delta_{\mu\eta}x}\,dx \quad , \tag{3.12}$$

where

$$\Delta_{\mu\eta} = \gamma_\eta \cos\psi_\eta - \gamma_\mu \cos\psi_\mu \tag{3.13}$$

On each of the grooves of the grating the amplitude change is small but in the case of phase synchronism the diffracted by the whole grating wave amplitude can become comparable with the incident one. Using the periodicity of the corrugation in x, (3.12) can be represented as:

$$h\,\Delta_{\mu\eta}\sum_m \frac{\gamma_m}{\Delta_{\mu\eta,m}d}\left[e^{i\Delta_{\mu\eta,m}d} - 1\right] \tag{3.14}$$

where

$$\gamma_m = \frac{1}{hd}\int_0^d f(x)\; e^{-imKx}\,dx \quad ,$$
$$\Delta_{\mu\eta,m} = \Delta_{\mu\eta} - mK \quad , \quad m = 0, \pm1, \pm2, \ldots \tag{3.15}$$

Considering the Bragg diffraction case, the only significant term in the sum (3.14) is the one with a slight deviation from the phase synchronism condition ($\Delta_{\mu\eta,m}\approx 0$), and equation (3.14) becomes equivalent to $ih\Delta_{\mu\eta}\gamma_m \exp(i\Delta_{\mu\eta,m}x)$. Substituting $\Delta a_\mu/d$ with $\partial a_\mu/\partial x$ (possible due to the small amplitude change on a single groove), the well-known system of coupled mode equations is obtained:

$$\begin{cases} \dfrac{da_\mu^j}{dx} = i\,\Gamma_{\mu\eta}^{j1}\, a_\eta^1\, e^{i\Delta_{\mu\eta,m}x} \\ \dfrac{da_\eta^1}{dx} = i\,\Gamma_{\eta\mu}^{1j}\, a_\mu^j\, e^{-i\Delta_{\mu\eta,m}x} \end{cases} \tag{3.16}$$

The coupling coefficients Γ are

$$\Gamma_{\mu\ \eta}^{TE\ TE} = \frac{h}{2}\gamma_m k^2 \frac{n_2^2(0)-n_1^2(0)}{2\omega\mu_0}\,\varepsilon_{\mu t}^*(0)\,\varepsilon_{\eta t}(0)\,\frac{\cos(\psi_\eta-\psi_\mu)}{\cos\psi_\mu} \quad . \tag{3.17}$$

$$\Gamma_{\mu\ \eta}^{TM\ TM} = \frac{h}{4\omega\varepsilon_0 \gamma_m}\left[\frac{1}{n_1^2(0)}-\frac{1}{n_2^2(0)}\right]\chi^*_{\mu t}(0)\chi_{\eta t}(0)\frac{\gamma_{TM\mu}\gamma_{TM\eta}+q_\mu q_\eta \frac{n_2^2(0)}{n_1^2(0)}\cos(\psi_\eta-\psi_\mu)}{\cos\psi_\mu}, \qquad (3.18)$$

where $q_\mu^2=\gamma_{TM\mu}^2 - k^2 n_1^2(0)$, and $\varepsilon(0)$ and $\chi(0)$ are the values of TE and TM mode eigenfunctions, calculated on the waveguide surface.

The case with a polarization conversion is more complicated due to the non-orthogonality of the longitudinal and transverse mode eigenfunctions and a numerical treatment is required. 9 sets of parameters of a step refractive index waveguide were considered: $n_1=1$, $n_2=1.62$, $n_3=1.515$, $t=3$, 5, 10, 15 and 20 μm and $n_1=1$, $n_2=2.234$, $n_3=2.216$, $t=6$, 10, 20 and 60 μm, including mono and multi mode cases (up to 8 modes). Within a 5% relative error the coupling coefficients can be approximated with the following expression:

$$\Gamma_{\mu\ \eta}^{TE\ TM} = \frac{h}{4}\gamma_m q_\eta n_2^2(0)\left[\frac{1}{n_1^2(0)}-\frac{1}{n_2^2(0)}\right]\varepsilon^*_{\mu t}(0)\chi_{\eta t}(0)\frac{\sin(\psi_\mu-\psi_\eta)}{\cos\psi_\eta}. \qquad (3.19)$$

Formulas (3.17) and (3.18) are valid for an arbitrary refractive index and groove profiles. (3.19) is valid for an arbitrary grating profile, too. For the case of normal incidence they coincide with the results of the local mode approach and of the "growing-wave" analysis of Stegeman et al. [114]. For oblique incidence, however, our results differ slightly from those of Stegeman et al. by the cosine in the denominator, responsible for the interaction length $l=d/\cos\psi$ for one groove.

In many cases the modulation depth is not very small compared to the period (e.g. grating in- and output couplers), but not big enough to modify significantly waveguide mode structure. When $h/d\leq 0.15$ it is possible to use the phenomenological approach. These methods could be divided into two groups with respect to the field representation:

1. Based of Rayleigh hypothesis (plane wave expansion) [111-113]. This is a very simple method, but it has two disadvantages - validity only for step-index waveguides and bad convergence rate for non-sinusoidal grating profiles.

2. Modal methods - solution of rigorous boundary problem is searched numerically as a sum over modes of unperturbed waveguide (in general it can be graded index).

Other two groups of methods could be specified according to the way the coupling coefficients are calculated:

1. Numerical determination of mode propagation constant in the coupling region. After that coupling coefficients are calculated using the relation $\Gamma=2k\mathrm{Im}(\alpha^P)$ [47, 113].

2. Application of the phenomenological approach presented in §3 of Chapter two.

Comparison was made between the results obtained using the last method and using analytical formulas (3.17) - (3.19). A very good coincidence is observed for three- and multilayered waveguides in the case of shallow corrugation when formulas (3.17) - (3.19) are valid.

Although in the numerical treatment rigorous electromagnetic theories can be used, they presume an approximation which is fulfilled if groove depth is small compared to the waveguide thickness - influence of the corrugation on mode propagation constants away from phase matching conditions is negligible. When the grating is deep enough, mode propagating constants are changed significantly even without mode interaction. Moreover, coupling becomes strong even when phase matching is not ensured. In that case different modes of the corrugated waveguide do not correspond at all to the modes of planar system. The only possibility is to search for a rigorous solution for energy transfer in different directions in waveguiding layer, substrate and cladding [105, 114, 115].

PART TWO: ANOMALIES IN BARE METALLIC GRATINGS

This part of the thesis contains a detailed study of different anomalies in diffraction characteristics of bare metallic gratings. Thin dielectric layer on the metallic substrate does not lead to new anomalies but to a slight shift of their position, depth and half width. Thicker layers could support leaky waveguide modes, excitation of which could lead to appearance of new anomalies, like resonance anomalies in corrugated dielectric waveguides (Part three). These anomalies in metallic gratings covered with a dielectric layer are studied in details and we should not discuss them.

The following remark has to be mentioned here: Further on appearance of curls in energy flow distribution is discussed in details. Usually existence of curls in vector field (of a vector A) means that rotA≠0. This is not the case with Poynting vector P of electromagnetic field in lossless media free of charges and currents: rotP≡0. By 'curls' for the sake of brevity we are naming regions of closed vector lines.

CHAPTER FOUR: LITTROW MOUNT ANOMALIES - PERIODICITY OF PROPERTIES AS A FUNCTION OF GROOVE DEPTH

It is well-known that there is a quasi periodicity of diffraction efficiency of grating supporting two diffraction orders. Existence of very high efficiency in Littrow mount is accompanied by a zero of the zeroth reflected order. Effort of Hessel and Oliner [28] to explain this 'anomaly' (called perfect blazing in Littrow mount or Bragg type anomaly) by surface wave excitation failed and later they proposed another interpretation - zeroth order zeros in Littrow mount are connected with improper poles of the scattering matrix. These poles are obtained when incident and reflected waves are exchanged, i.e. non-physical radiation conditions are implied. It is shown in the thesis that this correspondence between zeros of the reflected order and improper pole does not contain any explanation and happens always when incident and reflected waves are exchanged:

Mathematically this exchange is expressed as a change of the sign of incident wave vector component γ_0, perpendicular to the grating plane. If zeroth order amplitude is zero ($b_0^1=0$) for $\alpha_0=\alpha_0^2$ with non-zero incident wave ($a_0^i=1$) then formal exchange of incident and

reflected wave (carried out with the change of sign of χ_0) means that there is a reflected wave without an incident one, i.e. an eigensolution exists represented by a pole of the improper scattering matrix. This fact is of great importance for the results presented in the next two chapters, where it is shown that a close connection exists between resonance and non-resonance non-Littrow mount anomalies.

Tseng et al. [30] have shown that small variation of h around the value h_L responsible for perfect blazing moves the zero α_0^z in the complex α_0-plane along a trajectory perpendicular to the real axis. We were able to follow this trajectory in a very large groove depth interval and we found out that it is a straight line, tending towards minus imaginary infinity as grating tends towards flat surface (fig.4.1):

$$\alpha_0^z \longrightarrow \alpha_L - i\infty \quad . \tag{4.1}$$

This fact has two direct consequences that explain two well-known hypotheses:

1) Up to now it was assumed that perfect blazing in Littrow mount is a phenomenon, different from other anomalies. And indeed, resonance anomalies are localized for flat surfaces near the real α_0-axis - their position corresponds with surface wave propagation constants,

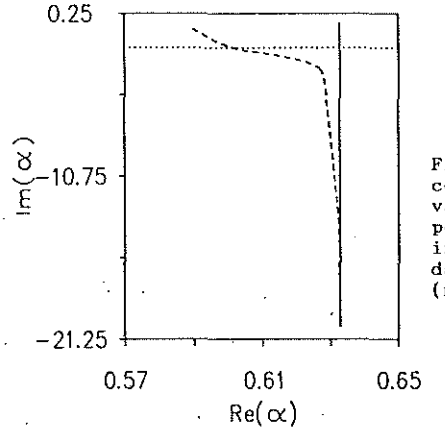

Fig.4.1. Trajectory of α^z in the complex α-plane when groove depth is varied: d=0.5 μm, λ=0.6328 μm, TM polarization. Solid line - infinitely conducting substrate, dashed line - aluminum grating (n=1.378+i7.616), dotted line- real axis.

while the 'starting' point of Littrow mount perfect blazing lies in $-i\infty$.

2) Littrow mount anomalies appear only in deep gratings, when α_0^z approaches the real axis and has some influence on diffraction efficiencies.

Increasing the groove depth, α_0^z approaches the real axis with rate determined by the following connections:

$$\begin{cases} \mathrm{Re}(\alpha_0^z) = \alpha_L \\ \frac{2\pi}{\lambda}\,\mathrm{Im}(\alpha_0^z)\, f_{-1} \approx -1 \end{cases}, \qquad (4.2)$$

where f_{-1} is the -1st Fourier component of grating profile function. These equations are fulfilled only till the zero is lying away from the real axis. When $\mathrm{Im}(\alpha_0^z)$ becomes small enough its decresing rate depends on the polarization. For a fixed value of h it crosses the real axis - perfect blazing in the -1st order appears. After that $\mathrm{Im}(\alpha_0^z)$ increases in a positive direction, zeroth order efficiency is growing and -1st order efficiency decreases.

Physical explanation of these peculiarities could be found on a microscopical level. Above a flat perfectly conducting surface energy flow is parallel to the surface. Its intensity is zero at equidistant planes. Their position above the surface is determined by the equations:

$$y_0^{TM} = (2m+1)\,\frac{\pi}{2k\gamma_0}, \quad m = 0, 1, 2, \ldots \qquad (4.3a)$$

for TM polarization, and

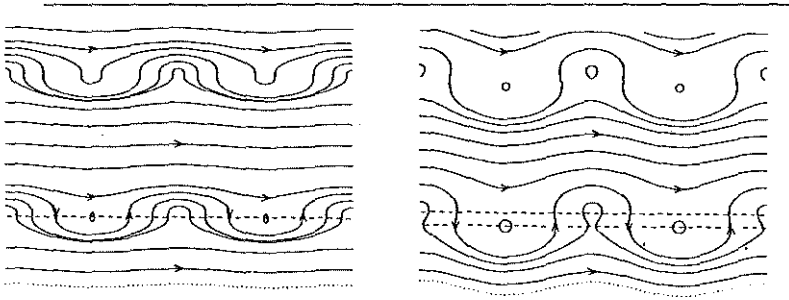

a b

Fig.4.2. Energy flow distribution:
(a) h/d=0.02, (b) h/d=0.08.

$$y_0^{TE} = 2m \frac{\pi}{2k\gamma_0} \quad , \quad m = 0, 1, 2, \ldots \quad . \qquad (4.3b)$$

for TE polarization.

For small corrugation, the lines (that represent the cross-section of energy flow surfaces with plane perpendicular to the grating) in the near vicinity of the surface are parallel to it (fig.4.2a). Vertical component of Poynting vector P_y becomes different from zero except for the positions above the tops and bottoms of the grooves. In the thesis it is shown that each plane, defined by eq.(4.3) is split into two, the splitting increases with h. Between each couple of planes P_x has a negative sign (fig.4.2b). As a result curls are formed around the points where $|P|=0$. Increasing groove depth, area occupied by the curls increases. They block energy flow in positive x direction increasing -1st order efficiency. It is important

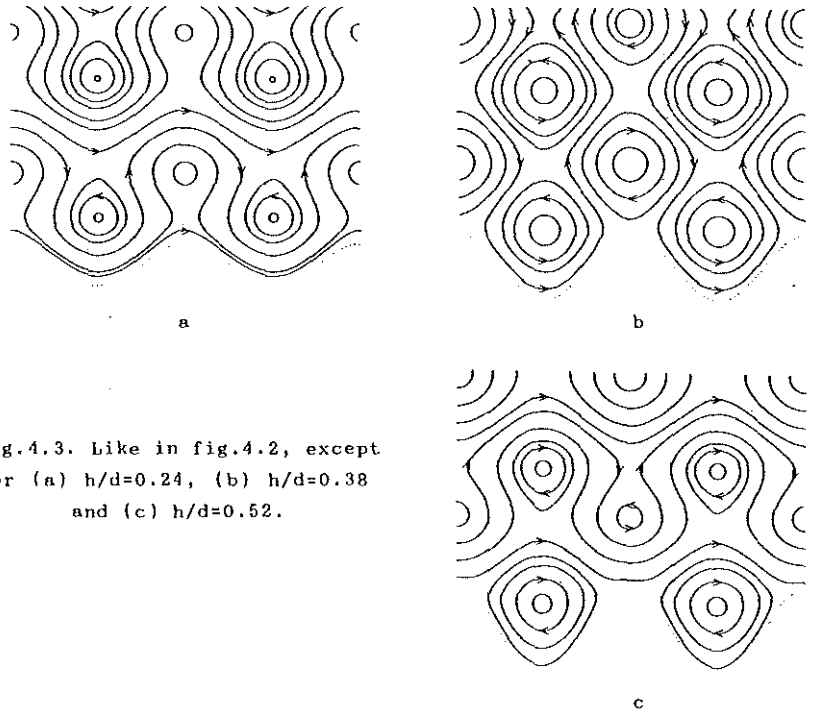

Fig.4.3. Like in fig.4.2, except for (a) h/d=0.24, (b) h/d=0.38 and (c) h/d=0.52.

to note that independent of groove depth value the centers of the lowest curls are situated at almost the same distance from grating surface. When the centers of the lowest bottom curls lie on the line connecting the groove tops, the entire upper medium is occupied by curls - there is now energy transfer towards reflected wave, i.e. perfect blazing in Littrow mount occurs. Taking into account eq.4.3, groove depth values responsible for perfect blazing are determined by:

$$h = y_0^{TE,TM} \quad . \qquad (4.4)$$

This equation is an approximation, but a rather good one - numerical results almost coincide with it. Moreover, it provides an explanation why perfect blazing in TE polarization is achieved at almost twice deeper gratings (compare eq.4.3a and 4.3b).

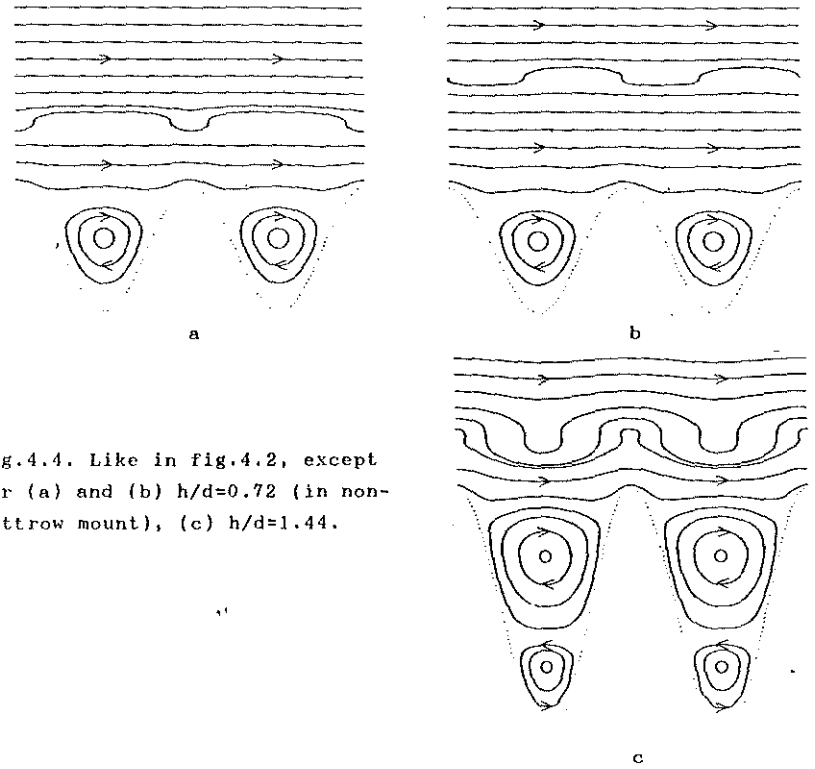

Fig.4.4. Like in fig.4.2, except for (a) and (b) h/d=0.72 (in non-Littrow mount), (c) h/d=1.44.

Further increase of groove depth causes bottom curls to go deeper and deeper. The distance between the centers of bottom and top curls decreases and they are unfolded - energy flow in positive direction increases. Energy flow distribution becomes more and more alike the distribution above shallow gratings, but only outside the grooves. When $h \approx 2y_0$ the centers of the top and bottom curls lie on one and the same line (fig.4.4a) and curls above the groove tops disappear. In that case the grating acts like a plane mirror. Inside each groove there is a totally hidden curl that separates energy flow above the grating from the groove bottoms. These curls are very stable - changing angle of incidence in a large interval causes no change in the flow distribution. This property called 'antiblazing' [118] is important for some effects discussed in the next two chapters.

Increasing groove depth leads to a repeating of fig.4.2 to fig.4.4 process, except for the lowest curls going deeper and deeper. Perfect blazing followed by antiblazing etc. could be detected (fig.4.4c) again.

It is shown in the thesis that when the grating supports a single order, in the near zone curls are formed periodically in the same manner like in figs. 4.2 - 4.4. They lead to a periodical behavior of the phase of reflected wave. It must be pointed out that perfect conductivity is not a limitation neither of the method nor of the results - it is assumed in order to make the picture of flow distribution more clear as there are no lines finishing at the surface. For finitely conducting gratings the behavior of flow distribution is almost the same. Moreover, in chapter 9 it is demonstrated that such formation of curls is typical for some peculiar cases of light diffraction by dielectric gratings, too.

CHAPTER FIVE: RESONANCE ANOMALIES IN METALLIC GRATINGS

Quasi-periodicity of properties of metallic gratings in Littrow mount, discussed in details in the previous chapter is a general property of gratings - it appears for other incident angles and even in grazing incidence (fig.5.1). Moreover, diffraction losses of surface plasmon that propagates along the corrugated metal-air interface are quasi-periodical function of groove depth. These losses were determined solving the homogeneous problem and the ratio between energy flow carried by the radiation order and by the surface wave. It

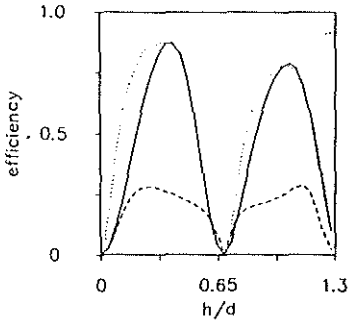

Fig.5.1. Diffraction characteristics as a function of groove depth: solid line - Littrow mount efficiency, dashed line - efficiency for α=0.99 and dotted line - diffraction losses of surface plasmon.

is shown in the thesis that the quasi-periodicity of the losses is due to formation of curls inside the deep grooves. As a direct consequence, there is a quasi-periodicity of imaginary part of plasmon propagation constant and loops are formed in its trajectory in the complex α_0-plane as a function of groove depth (fig.5.2). In the regions where $|\mathrm{Re}\alpha^p|<1$ eigenvalue is transferred into a zero of the zeroth order amplitude α_0^z - large losses lead to delocalization of surface wave.

Some points of the trajectory of fig.5.2 lead to anomalies that are discussed in the next chapter. They appear in the regions $|\mathrm{Im}\alpha^p|<1$ where there is no surface wave and are of non-resonance type.

It is well-known that grating multiplies the poles [19, 20]. In particular, similar loops are formed near the point $1-\lambda/d$ due to plasmon excitation through the +1st diffraction order. In that case the existence of pole is accompanied by a zero. When this zero lies near the real α_0-axis the reflection of the grating is very small - total absorption of light can occur under certain conditions. This phenomenon was discovered by Maystre and Petit in 1976 [38] for

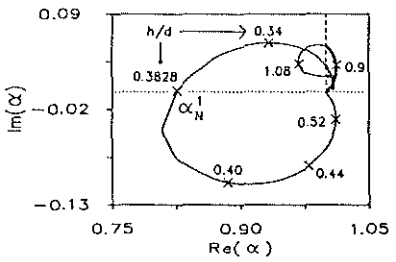

Fig.5.2. Trajectory of α^p (heavy line) and of α^z (thin line) when groove depth is increased. The cut in the complex plane that corresponds to the change of sign of χ_0 [121] is presented with dash line.

Fig.5.3. Energy flow distribution in the three cases of total absorption of light by aluminum grating: (a) h/d=0.1, θ=14.82°. (b) h/d=0.79, θ=14.93°. (c) h/d=1.2, θ=15.06° [132].

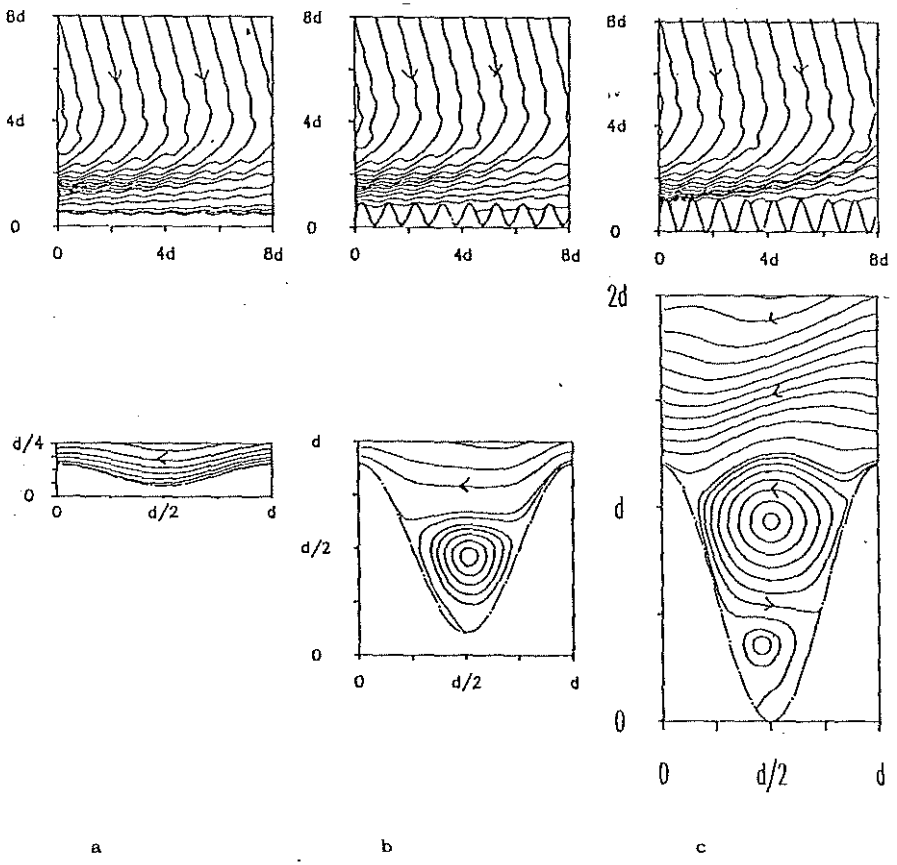

shallow gratings. In the thesis it is shown that total absorption occurs in deep gratings as well. For aluminum grating it happens three times when the groove depth is increased (h/d=0.1, 0.69 and 1.2). In deep gratings there are one or two curls in each groove that separate energy flow above the tops from groove bottoms. Just above the tops

energy flow distribution is one and the same in the three cases (fig.5.3). Flow lines are turning to the negative direction of x-axis, corresponding to surface wave excitation through the -1st diffraction order. The lines are compressed resulting in enhancement of local

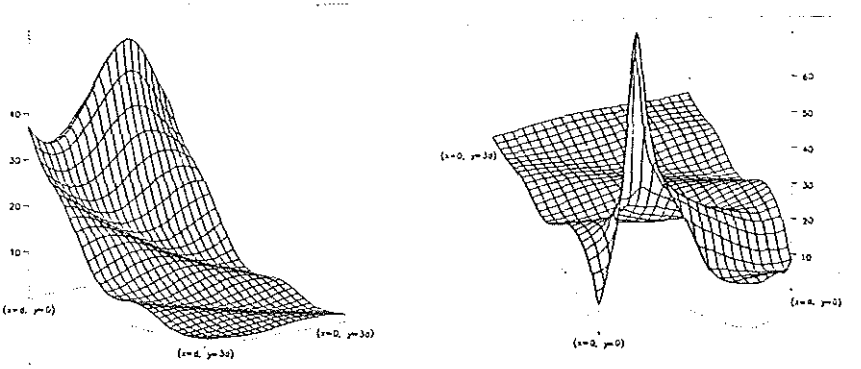

a b

Fig.5.4. 2-D distribution of electromagnetic field energy, corresponding to fig.5.3a and b.

electromagnetic field energy. Such enhancement was well-known for total absorption of light in shallow grating and was utilized in nonlinear second harmonic excitation [123 - 127] and luminiscence [128] and SERS [129 - 131]. We have shown that total absorption of light is accompanied by field enhancement in deep gratings, too. Due to the peculiar behavior of energy flow (compression of lines above the tops is separated from the bottoms), field enhancement now is localized only on the tops of the grooves (fig.5.4).

Diffraction efficiency anomalies in the -1st order of aluminum grating in conical diffraction are discussed in the last section of chapter five. As this anomaly is well investigated, our interest is attracted by the occurrence of anomaly in TE fundamental polarization when going away from the in-plane case (fig.5.5). In classical case ($\varphi = 0$) the incident wave vector is perpendicular to the grooves. TE polarized wave has an electric field vector perpendicular to the plasmon electric vector and there is no anomaly due to plasmon excitation (fig.5.5a). As angular deviation from in-plane case is growing, anomaly appears in TE polarized light as well. The dip in the

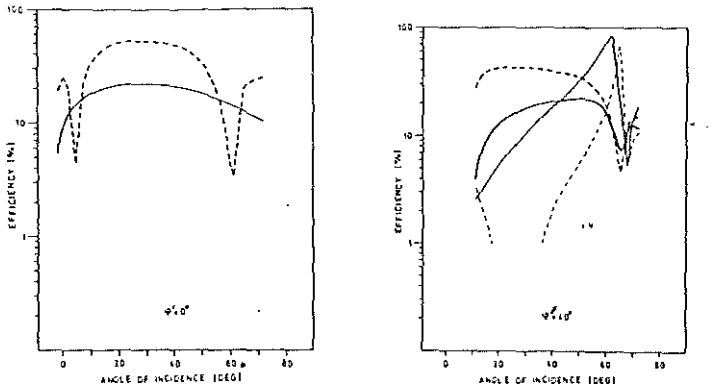

Fig.5.5. Experimental angular dependence of diffraction efficiency (heavy line) and ellipticity (thin line) for different angular deviation φ' from classical diffraction case. Solid line - TE polarization, dashed line - TM polarization.

angular dependence (varying the other angle of incidence) for TM polarization decreases and for TE polarization deepens (fig.5.5b). Interesting phenomenon is a sharp increase of ellipticity of diffracted wave in the anomalous region, although incident wave is linearly polarized.

CHAPTER SIX: NON-RESONANCE ANOMALIES IN METALLIC GRATINGS IN NON-LITTROW MOUNTING

The main difference between resonance and non-resonance anomalies appears in electromagnetic energy distribution - resonance anomalies are characterized with large (one order and more) field enhancement in the vicinity of grating surface, while in the case of non-resonance anomalies such phenomenon is not observed. From a phenomenological point of view resonance anomalies are connected with a pole of the scattering matrix. This pole is usually accompanied by a zero of the corresponding diffraction order amplitude, but the pole is responsible for resonance field enhancement. Non-resonance anomalies are due to appearance of a zero without a pole. One such anomaly was considered in chapter four - zeroth order zero in Littrow mount that lead to perfect blazing in the -1st order. This anomaly is not accompanied by a pole - the trajectory of the zero starts from $-i\infty$ for

flat surface. The anomalies discussed in this section are of another type - they are also due to a zeroth order zero without a pole, but the trajectory of such a zero alternatively consists of poles (fig.5.2). We should now consequently discuss some peculiar points of this trajectory. It is obvious that such anomalies appear only for TM polarization in the case of bare metallic gratings.

Often diffraction gratings are used in grazing incidence for improving grating dispersion. Unfortunately as angle of incidence tends to 90° the zeroth order efficiency tends to unity and -1st order efficiency rapidly decreases. Numerical optimization of blazed and sinusoidal aluminum gratings was done [139] and the results could be summarized as follows:

1. Sinusoidal profile is preferable when grating supports two diffraction orders.
2. Increase of groove density leads to a higher diffraction efficiency, but shifts the working spectral region towards shorter wavelength and increases sensibility to groove depth values.
3. Diffraction efficiency in TM polarization exceeds more than 10 times the efficiency in TE polarization.
4. Maximum efficiency in grazing incidence is obtained at about 20% modulation depth (fig.6.1), while in Littrow mount the corresponding h/d value is 40%

The last two properties could easily be understood just following the trajectory of fig.5.2. Let us fix the view point at $\alpha_0 = \sin 89°$. The real part of α_0^z becomes almost equal to α_0 when h/d≈0,22. Then a maximum in the -1st order efficiency could be

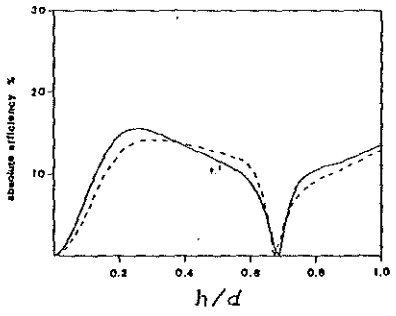

Fig.6.1. Diffraction efficiency vs. modulation depth h/d - sinusoidal Al grating, angle of incidence 89°.

expected. Its value is determined mainly by $Im(\alpha_0^z)$ and when absorption losses in the metal are growing $Im(\alpha_0^z)$ becomes greater and -1st order efficiency decreases. As far as such a trajectory (fig.5.2) is typical only for TM polarization and for TE polarization there is no zeroth order zero lying in the vicinity of α_0, TM -1st order efficiency is much higher.

Further increase of h/d moves α_0^z away from $\alpha_0=\sin 89^\circ$, zeroth order amplitude increases (as it depends on the difference $\alpha_0-\alpha_0^z$) and -1st order efficiency decreases (fig.6.1). Because the trajectory of the zero α_0^z is almost parallel to the real α_0 axis when h/d~0.2, groove depth dependence of efficiency is rather smooth. This fact could be of great practical interest as it is very difficult to produce a grating with preliminary fixed groove depth.

Tracing the trajectory with increase of groove depth, it crosses the real axis when h/d~0.39. The cross-point α_{N1}^z corresponds to the so-called 'perfect blazing in non-Littrow mount' discovered in 1980 [37]. We were able to find its proper explanation (fig.5.2) and to show why perfect blazing in TE polarization exists only in Littrow mount. It is interesting to note that perfect blazing in Littrow and non-Littrow mount are exhibited at almost one and the same groove depth values thus angular interval with high diffraction efficiency is enlarged. The results are quite different for two polarizations (fig.6.2):

1. TM polarization (h=0.194μm, d=0.5μm). Three zeroth order zeros are found at $\alpha_0=0.82$ (α_{N1}^z), 0.63 (α_L^z) and 0.44 (symmetrical to α_{N1}^z with respect to α_L^z). Thus zeroth order efficiency is almost zero in a large

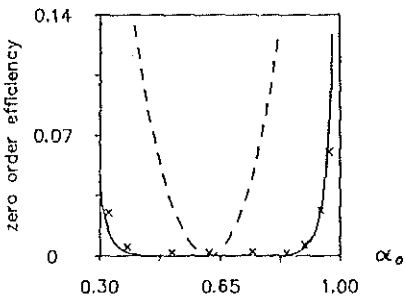

Fig.6.2. Zeroth order efficiency as a function of $\alpha_0=\sin\theta_0$. Solid line - TM polarization, h/d=0.388, dashed line TE polarization, h/d=1.32. $\lambda/d=1.2656$.

angular interval leading to high (>85%) efficiency in the -1st order. 2. TE polarization (h=0.66μm, d=0.5μm). There is no perfect blazing in non-Littrow mount and the angular interval with low zeroth order efficiency is much narrower.

With further increase of h/d the trajectory of α_o^z crosses again the real axis again at α_c=0.9993 (fig.5.2 and 6.1 with h/d=0.69). Zeroth order efficiency again becomes nil. Efficiency in the -1st order depends on the groove profile. Symmetrical triangular profile results in very high efficiency (fig.6.3b and 6.4b). Unfortunately groove depth is very large (h/d=0.69). For sinusoidal profile with that groove depth value -1st order amplitude is almost zero in a large angular interval ('antiblazing' of gratings [141]) and, in particular, in grazing incidence (fig.6.3a and 6.4a). Superposition of those two phenomena (zero of the zeroth and -1st

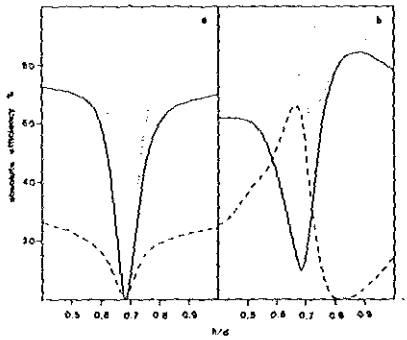

Fig.6.3. Diffraction efficency in the 0-th (solid line) and -1st (dashed line) order and total diffracted energy (dotted line) as a function of modulation depth h/d for Al grating with (a) sinusoidal, and (b) symmetrical triangular profile. d=0.5 μm, λ=0.6328μm, TM polarization, θ=87.85°.

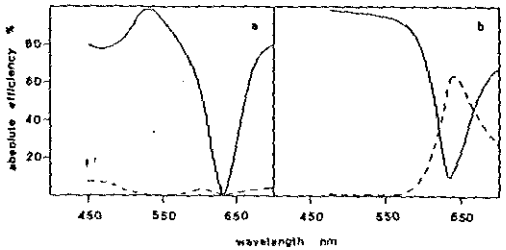

Fig.6.4. Like Fig.6.3, but as a function of wavelength when h/d=0.69.

order amplitudes) lead to almost total absorption of incident light by a grating supporting two diffraction orders. It appears when the trajectory of α_0^z in fig.5.2 lies to the left of the cut and there is no pole. That is why there is no field enhancement - this anomaly is of non-resonance type. Contrary to the cases of total absorption discussed in Chapter 5 now there is no surface wave excitation and energy flow lines are not compression of flow lines near the grating surface.

CHAPTER SEVEN: ANOMALIES INTERACTION IN METALLIC GRATINGS

This chapter deals with the influence of simultaneous appearance of two anomalies on the diffraction characteristics. It is well known that interaction of eigensolutions lead to splitting and repelling of trajectories of the corresponding eigenvalues due to orthogonality requirements. Such a behavior is characteristic not only for the poles of the scattering matrix, but of zeroth reflected order zeros as well, as shown in §1. The reason is that these zeros are in a peculiar manner eigenvalues, but of the non-physical problem (Chapter four). Such an interaction between the trajectories of the zeros is quite important, as far as in many of the anomalies the influence of the zeros is greater than that of the poles.

Simultaneous excitation of two oppositely propagating surface plasmons along shallow gratings and its influence on anomalies in reflectivity is discussed in §2. Energy transfer between the two surface waves leads to a sharp increase of imaginary parts of their propagation constants. The pole moves away from the real axis and surface wave excitation becomes more difficult and anomaly dip in the reflectivity becomes less noticeable in thespectral interval corresponding to the interaction region - the so-called forbidden ω-mini gap is formed.

It was shown in 1987 [145, 146] that under certain conditions k-mini gap could be formed - interval of angles of incidence where anomaly is not so manifested. Tran et al. [147] found a connection that determined the formation of a definite type of gap depending on the ratio between radiation and absorption losses and direct coupling strength between the two surface waves. Our aim was to find the physical background of this link. For that sake a tracing of trajectories of zeros and poles as a function of wavelength for

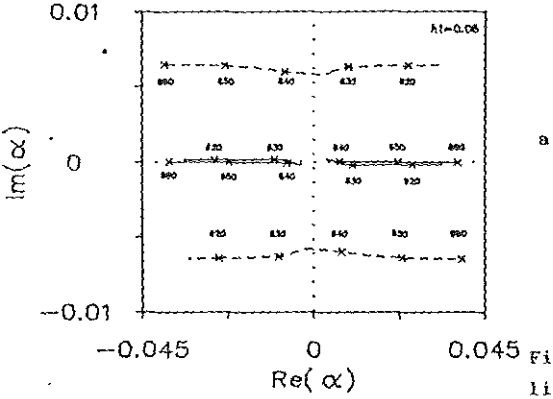

a

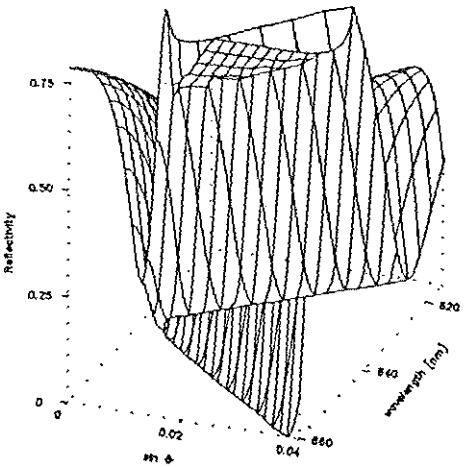

b

Fig.7.1 a) Pole (dashed lines) and zero (solid line) trajectories as a function of wavelength (shown in nm). Sinusoidal grating, h=0.06 μm. b) Corresponding wavelength - angle of incidence dependence of reflectivity.

fferent groove depth values and profiles is presented near normal cidence. Coupling between incident and surface waves is direct rough the ±1st Fourier components of grating profile $f_{\pm 1}$). Coupling ween oppositely propagating surface plasmons is of two types: ect (carried out through the second Fourier components of the file $f_{\pm 2}$, if any) and indirect (through $2f_{\pm 1}$). We are dealing with

aluminum grating with period d=0.63 μm and profile function:

$$f(x)=\frac{h_1}{2}\sin\left(\frac{2\pi}{d}x\right)+\frac{h_2}{2}\sin\left[\frac{4\pi}{d}\left(x+q\,\frac{d}{8}\right)\right] \quad , \quad q=0,\ 1\ . \tag{7.1}$$

If q=0 then f(x) is anti symmetrical, and if q=1 - symmetrical. At first h_2 is nil and coupling between incident and surface waves is much stronger than between the surface waves, provided the grating is shallow. Thus the repelling of trajectories of the poles (fig.7.1a) is determined predominantly by radiation and diffraction losses, but not

---

Fig.7.2. Like fig.7.1, except fo profile given by eq. (7.1) with h_2=0.02 μm.

a

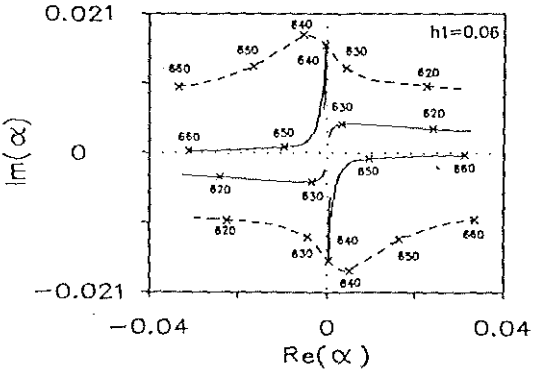

b

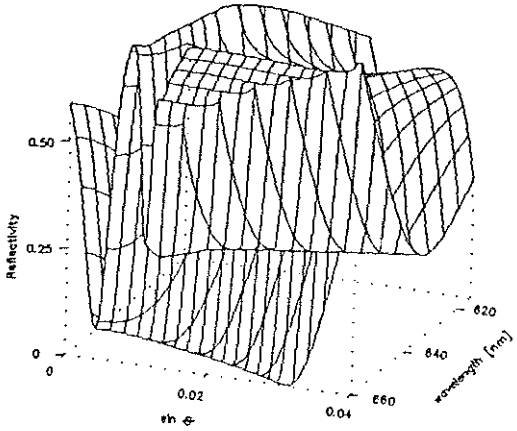

by a plasmon coupling even near normal incidence. Similar behavior have the zeros except for the groove depth value h_1=0.06 μm. Then their trajectories are lying near the real axis and in the vicinity of α_0=0 their separation becomes so small that even weak indirect coupling leads to the repelling: angular interval around α_0=0 exists without real zeros, the value of minimum in the reflectivity increases and k-mini gap is formed (fig.7.1b).

It has to be pointed out that existence of forbidden gap for the anomaly in the reflectivity in this case does not correspond to a forbidden gap in the surface plasmon propagating constant α^p - pole trajectories do not exhibit any noticeable peculiarities. Thus it could be risky to determine the values of real and imaginary part of α^p from experimental results for position, half width and minimum value of the reflectivity dip.

When direct coupling between surface waves is greater ($h_2 \neq 0$) repelling of the pole trajectories appears (fig.7.2a), practically independent on the strength of indirect coupling. In agreement with general theoretical principles, strong interaction between zeros could be found, too. In the vicinity of α_0=0 trajectories of the zeros approach the trajectories of the poles and mutual annihilation leads to a formation of spectral interval without anomalies - ω-mini gap region appears (fig.7.2b). A peculiar mechanism of transition between two types of gaps with the increase of h_2 is discussed in the thesis.

Anomaly interactions in deep metallic gratings is analyzed in §3. For shallow grooves repelling of trajectories could be noticed only in the near vicinity of their "intersection" points. For deep gratings interaction region is much larger. It is shown in the thesis how different types of coupling between poles and zeros determines short- and long-wavelength limits of different anomalies:

1. Brewster's effect (resonant total absorption of light) in deep gratings exists when $\lambda/d \in (1.19, 1.40)$. Decreasing the wavelength, the loops in the trajectory of the zero shrink in the vicinity of α_0=0. Thus the groove depth interval with high absorption values increases (vertical part of the dependence in fig.7.3 and 7.4).
2. Perfect blazing in non-Littrow mount exists for $\lambda/d \in [1.04, 1.48)$.
3. Grazing incidence zeroth order zero could be found in large spectral interval $\lambda/d \in (1.04, 2)$, but it leads to almost total absorption of light only when it is accompanied by a -1st order zero

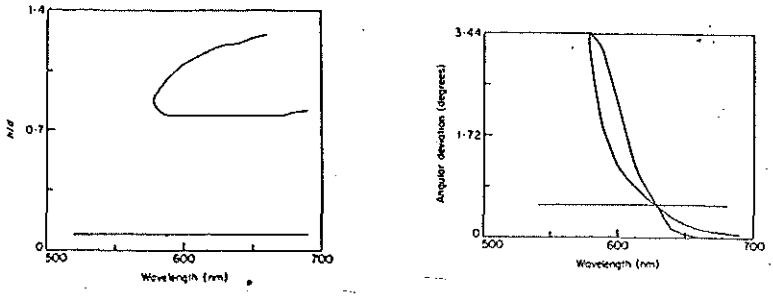

a b

Fig.7.3.Spectral dependence of groove depth values (a) and angula deviation from -1st order cut-off (b), corresponding to total ligl absorption in shallow and deep aluminum grating.

(for aluminum sinusoidal grating it happens when $\lambda/d=1.2656$)

PART THREE: ANOMALIES IN DIELECTRIC GRATINGS

CHAPTER EIGHT: RESONANCE ANOMALIES IN CORRUGATED OPTICAL PLANAR WAVEGUIDES

In multilayered dielectric gratings resonance anomalies are due to guided wave excitation. Two are the main differences with bare metallic gratings:

1. Corrugated waveguides can support both TM and TE modes thus resonance anomalies appear in both polarizations.
2. Much smaller value of losses in optical dielectric waveguides compared to metallic substrate enables the existence of pole α^P to manifest itself rather more noticeably - anomalies consist of peaks and dips, contrary to resonance anomalies in metallic gratings where these peaks could not be detected or are rather weak.

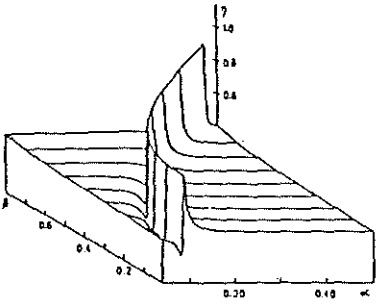

Fig.8.1. Reflectivity in conical mounting of corrugated wavefuide. $n_1=n_3=1$, $n_2=2.3$, $t=0.1\mu m$, $d=0.3\mu m$, $h=0.04\mu m$, $\lambda=0.6\mu m$, unpolarized light.

The peak is much more pronounces when it is accompanied by a low valued background. Most peculiar is the behavior of reflectivity (fig.8.1). Two cases are discussed in the thesis in details - grating supporting only the zeroth orders in the cladding and in the substrate, and having more diffraction orders. Phenomenological approach makes it possible to draw some general rules connecting symmetry of the system with the main characteristics of anomaly, provided only the zeroth orders are propagating:

(a) symmetry with respect to horizontal axis (e.g. symmetrical waveguide with anti-symmetrical groove profile on upper and lower boundary) - reflectivity minimum is always zero.

(b) symmetry with respect to vertical plane (e.g. asymmetrical

waveguide with symmetrical corrugation) - reflectivity maximum reaches 100%, at least theoretically.

(c) symmetry with respect to horizontal plane (it is difficult to produce such a waveguide) - reflectivity changes from 0 to 100% in the anomalous region.

Of course, these conclusions are valid only for lossless waveguides and for plane incident wave.

§2 presents experimental results of resonance anomaly in graded-index waveguide. After a grating with 0.3 μm period was recorded interferometrically in a layer of positive photoresist Shipley AZ1350, it was transferred into the glass substrate using ion-beam milling. Monomode waveguide was made in the corrugated substrate using ion-exchange in molten $AgNO_3$. Angular and spectral dependencies of reflectivity in the region of waveguide mode excitation are shown in fig.8.2. Half width of the maximum is about 3 nm - much narrower than the other tunable reflection optical filters.

If the period of the grating is larger and higher orders are propagating, the rules that are connecting the properties of anomaly with symmetry of the system are valid only for shallow grooves. A demonstration of this fact is presented in §3 of chapter 8. It is

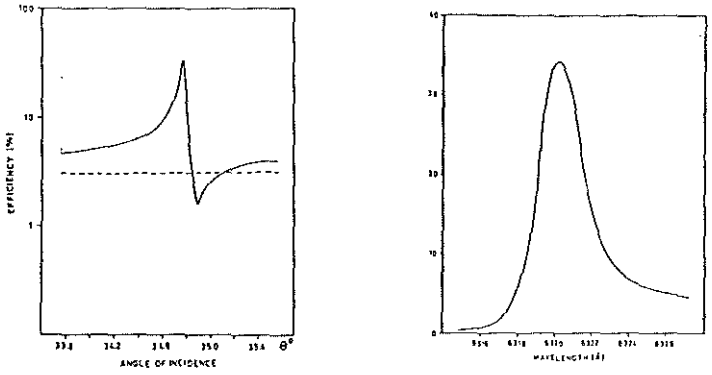

a b

Fig.8.2. Angular (a) and spectral (b) dependance of reflectivity of dielectric grating. Dashed line - without waveguide, solid line - after the ion-exchange.

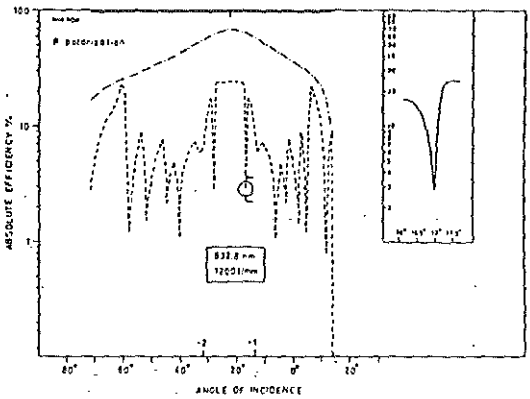

Fig.8.3. Angular dependence of -1st order efficency (TE polarization, λ=0.6328 μm). -.-.- - Al grating, ---- - multilayered dielectric grating, —— - plane dielectric muirror [154].

interesting to note that for shallow grooves waveguide mode excitation is accompanied by a peak in the efficiency of non-zero orders, but these peaks are only a few percent high. It is possible, in principle, to increase drastically the efficiency in reflected orders by increasing groove depth and imposing a multilayered dielectric reflection coating upon grating surface. Unfortunately from a practical point of view, a coating with optical thickness enough to increase significantly reflectivity and diffraction efficiency could support great number of waveguide modes. Contrary to the planar case, grating enables to excite these modes by a plane incident wave - a lot of resonance anomalies appear as deep minima (fig.8.3). In the thesis a detailed study is presented for different wavelength values and polarizations. For example, decreasing the wavelength the number of anomalies increases due to the increase of number of modes and decrease of grating vector.

CHAPTER NINE: NON-RESONANCE ANOMALIES IN DIELECTRIC GRATINGS

Another possible way to increase diffraction efficiency in reflected non-zeroth orders is to decrease the number of propagating diffraction orders. The best solution is to retain only two orders, as it is in the case of fine pitch metallic gratings. This is possible if the dielectric grating is used with light incident from the substrate

side under the angle higher than the critical one for total internal reflection. Provided the period is small enough, there is no propagating order in air and in the substrate only two orders exist. Like metallic gratings supporting two orders, highest diffraction efficiency is obtained in Littrow mount. Increasing groove depth, diffraction efficiency behavior is quasi periodical (fig.9.1), similar to the metallic grating (chapter 4). Here again a formation of curls in energy flow distribution is found that determines the efficiency behavior. As both media are dielectric, flow lines penetrate much deeper in the lower medium and are larger than the curls in metallic gratings. Thus groove depth value responsible for perfect blazing (when the center of the lowest curl is lying on the line connecting groove tops) is higher (fig.9.1) than for metallic gratings. This is a great limitation to the practical usage of such gratings - it is very

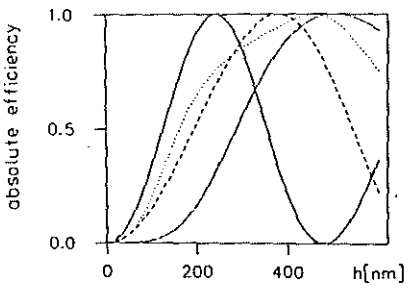

Fig.9.1. Groove depth dependence of -1st order efficiency of dielecric grating with light incident from the substrate side (n=1.5). Solid line - TE polarization поляризация (λ=0.550 μm), dotte curve - TM polarization (λ=0.550 μm); dashed line - TE polarization (λ=0.650 μm), border line - TM polarization (λ=0.650 μm). d=0.26 μm, Littrow mount.

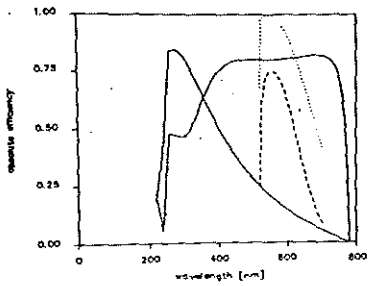

Fig.9.2. Spectral dependence of diffraction grating with refractive index of the upper medium 1.5. Secon medium is air (dotted line - TE polarization, dashed line - TM polarization), or aluminum (solid line - TE polarization, border line- TM polarization). d=0.26μm, h=0.24 μm, Littrow mount.

difficult to manufacture grating with small period (d~0.25 μm) and high modulation depth (h/d~1). The main advantage lies in the fact that here absolute efficiency could reach 100% value - losses are much lower than in metallic gratings.

Spectral dependence of efficiency in Littrow mount is presented in fig.9.2 for a fixed groove depth value. It looks like efficiency in TE polarization for metallic gratings and this could easily be understood taking into account that much broader maximum for TM polarization of metallic grating is due to the existence of non-Littrow perfect blazing (see chapter 6). This phenomenon is connected in a peculiar manner with existence of surface plasmon on bare plane metal-air interface. As far as such surface waves could not propagate along the interface between two dielectrics, non-Littrow perfect blazing is not detected in fig.9.2 for the case of dielectric grating.

CHAPTER TEN: ANOMALIES AND MODE INTERACTION IN CORRUGATED PLANAR WAVEGUIDES

This chapter presents results on two aspects of mode coupling in corrugated planar waveguides:

1. Influence of simultaneous excitation of more than one mode on the resonance anomalies.
2. Brewster's effect in corrugated waveguides - anomaly in the coupling coefficients of mode interaction in the corrugated region of a planar waveguide.

For multilayered planar waveguide it is possible to have differently polarized modes with equivalent propagation constants, provided the parameters are properly chosen. In §1 this possibility is utilized to obtain resonance anomalies in the reflectivity for the two fundamental polarizations - important when working in unpolarized light.

If phase conditions for mode excitation are satisfied near normal incidence, then two oppositely propagating modes are excited simultaneously. This mounting enables to use the narrow band reflection filter (chapter 8) directly as a selectable mirror (for example, in laser resonators). Anomaly interaction leads to appearance of two peaks. At a certain set of parameters annihilation of poles and zeros happens, like formation of ω-minigap in metallic gratings.

Fortinately, for symmetrical corrugation profile only one peak is formed in spectral dependence of the reflectivity.

Brewster's effect in corrugated planar waveguides is discussed in §3. When TE modes are coupled in a corrugated region of a planar waveguide, at a given angle between their directions of propagation the coupling vanishes. This phenomenon has been known for years, but there is nor proper understanding, neither a common opinion on this angle value.

The form of the angular dependencies in (3.17) - (3.19) has two direct consequences:

(i) co- and contra-linear interactions are carried out with a polarization conservation, and

(ii) if the angle between the directions of propagation is equal to $\pi/2$ the coupling between TE modes vanishes. From eq. (3.17) it follows that the effect is valid for both the coupling of modes with the same, and with different orders. Furthermore, even on a single step boundary (eq.(3.11)) TE mode coupling vanishes as the angular difference becomes 90°. As far as the existence of grating leads to a constructive (or destructive) interference between the diffracted on each groove modes, it is obvious that in the case of the zero coupling on a single boundary no interaction would appear throughout the whole corrugated region.

In the thesis it is shown that Brewster's effect in corrugated waveguides could be directly utilized to suppress the undesired depolarization in some integrated optical devices.
Schematically presented in fig.10.1 beamsplitter and polarizer consists of three gratings, the firs used for light coupling into the waveguide, and the other gratings are crossed under the angle of $\pi/2$. Measured depolarization in direction perpendicular to the initial

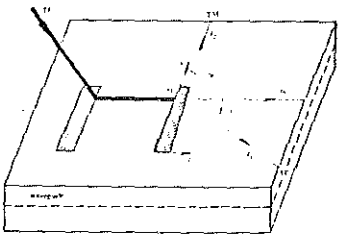

Fig.10.1. Schematical represntation of integrated-optical coupler, beam-splitter and polarizer, based on relief diffraction gratings upon a planar waveguide.

direction of propagation is less than 1% - only TE - TM mode conversion is observed, although mode propagation constants are almost one and the same for the two polarization and phase conditions are satisfied for excitation of both modes.

Increasing the groove depth, expressions (3.17)-(3.19) for the coupling coefficients obtained in the first order approximation are no longer valid and the use of the rigorous method becomes necessary. A monomode waveguide has been considered (n_1=1, n_2=2.3, n_3=1.6, t=0.07 μm). In order to avoid the influence of the other types of coupling, its thickness has been taken to be less than the TM mode cut-off. The numerical results are shown in fig.10.2 for a sinusoidal groove profile. As the corrugation depth is increased the effective refractive index of the mode is changed, too, because h becomes comparable to the waveguide thickness. Within a relative error of 0.1% it has been shown that even for deep gratings (h/t>0.5) the Brewster's law analogy exists; the value of the zero-coupling angle φ_B depends on the groove depth and for relatively small h its deviation from 45° is proportional to h^2 (fig.10.2), due to the invariance of the phenomenon to the change of the h sign.

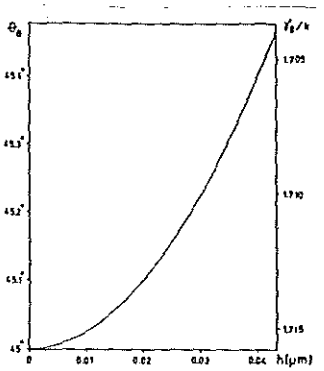

Fig.10.2. Groove depth dependence of TE mode propagation constant γ_B/k and Brewster's angle θ_B. λ=0.6 μm.

CONCLUSION

The present thesis is devoted to theoretical and experimental investigations on diffraction grating anomalies. Main results of the thesis could be grouped in the following directions:

I. Some new anomalies in diffraction efficiency of metallic and dielectric relief gratings are predicted theoretically and confirmed experimentally, as follows:

1. Resonance total absorption of light in deep metallic gratings supporting a single propagating order.

2. Non-resonance total absorption of light by metallic gratings with two propagating orders.

3. 'Antiblazing' of metallic gratings - diffraction efficiency of a deep metallic grating is almost zero in the entire angular interval, provided it is zero in Littrow mount.

4. Total delocalization of surface plasmon on corrugated metal-air interface when radiation (diffraction) losses are high - then eigensolution of the system is not existing.

5. Resonance anomaly in the reflectivity of corrugated waveguides.

6. 'Perfect blazing' for bare dielectric gratings when light is incident from the substrate side.

Some possibilities for utilization of these effects are discussed.

II. Connections are revealed that exist between these new anomalies and already known ones, as well as between known but unidentified anomalies ('perfect blazing' in Littrow and non-Littrow mount and Brewster's effect in shallow metallic gratings). Determination of such connections enables to identify different anomalies, i.e. to link them with (or to distinguish them definitely from) some phenomena on flat surfaces (waveguide modes in optical waveguides and surface plasmon wave on metal-air interface).

III. Physical reasons for appearance of anomalies are found in the behavior of electromagnetic field characteristics in the vicinity of grating surface and their influence on the far-field parameters. It is shown that curls are formed in energy flow distribution . At a given groove depth value the lowest curls are totally hidden inside the grooves and energy flow above the groove top is similar to the flow above flat surface - quasi-periodicity of phases and efficiencies of

the propagating orders and of the diffraction losses of surface wave is induced.

The results presented in the thesis are published in the following papers:

1) L. L. Konstantinov, I. Z. Kostadinov and E. K. Popov: "Photoelectricity of AgI Under SubBandgap Illumination," Sol. St. Ionics **8**, 127 (1983)
2) L. Mashev and E. Popov: "Diffraction efficiency anomalies of multilayer dielectric grating," Opt. Commun. **51**, 131 (1984)
3) L. Mashev, S. Tonchev and E. Popov: "Two Dimensional Grating Beam Splitter and Polarizer," Bulg. J. Phys. **12**, 297 (1985)
4) E. Popov and L. Mashev: "Dispersion Characteristics of Multilayered Waveguides," Opt. Commun. **52**, 393 (1985)
5) L. Mashev and E. Popov: "Zero Order Anomaly of Dielectric Coated Grating," Opt. Commun. **55**, 377 (1985)
6) E. Popov and L. Mashev: "Analysis of Mode Coupling in Planar Optical Waveguides," Opt. Acta **32**, 265 (1985)
7) E. Popov and L. Mashev: "The Determination of Mode Coupling Coefficients," Opt. Acta **32**, 635 (1985)
8) E. Popov and L. Mashev: "Convergence of Rayleigh Fourier Method and Rigorous Differential Method for Relief Diffraction Gratings," Opt. Acta **33**, 593 (1986)
9) E. Popov, L. Mashev and D. Maystre: "Theoretical Study of the Anomalies of Coated Dielectric Gratings," Opt. Acta **33**, 607 (1986)
10) E. Popov and L. Mashev: "Conical Diffraction Mounting: Generalization of a Rigorous Differential Method," J. Optics **17**, 175 (1986)
11) E. Popov and L. Mashev: "Diffraction Anomalies of Coated Dielectric Gratings in Conical Diffraction Mounting," Opt. Commun. **59**, 323 (1986)
12) E. Popov and L. Mashev: "Rigorous Electromagnetic Treatment of Planar Corrugated Waveguides," J. Opt. Commun. **7**, 127 (1986)
13) G. A. Golubenko, A. S. Svakhin, V. A. Sychugov, A. V. Tischenko, E. Popov and L. Mashev: "Diffraction Characteristics of Planar Corrugated Waveguides," J. Opt. Quant. Electr. **18**, 123 (1986)
14) E. Popov and L. Mashev: "Convergence of Rayleigh Fourier method and rigorous differential method for relief diffraction gratings nonsinusoidal profile," J. Mod. Opt. **34**, 155 (1987)
15) L. Mashev and E. Popov: "Reflection gratings in conical diffraction mounting," J. Opt. (Paris) **18**, 3 (1987)
16) E. Popov and L. Mashev: "Diffraction from planar corrugated waveguides at normal incidence," Opt. Commun. **61**, 176 (1987)
17) L. Mashev and E. Popov: "Phenomenological approach to the resonance anomalies in relief diffraction gratings," Bulg. J. Phys. **14**, 342 (1987)
18) L. Mashev and E. Popov: "Numerical Optimization of holographic diffraction grating efficiency," Bulg. J. Phys. **14**, 549 (1987)
19) L. B. Mashev, E. K. Popov and E. G. Loewen: "Asymmetrical trapezoidal grating efficiency," Appl. Opt. **26**, 2864 (1988)
20) L. B. Mashev, E. K. Popov and E. G. Loewen: "Total absorption of light by a sinusoidal grating near grazing incidence," Appl. Opt. **27**, 152 (1988)
21) L. B. Mashev, E. K. Popov and E. G. Loewen: "Optimization of the grating efficiency in grazing incidence," Appl. Opt. **26**, 4738 (1987)

22) E. Popov, L. Mashev and D. Maystre: "Backside diffraction by relief gratigs," Opt. Commun. **65**, 97 (1988)
23) L. Mashev, E. Popov and D. Maystre: "'Antiblazing' effect in gratings," Opt. Commun. **67**, 5, 321 (1988)
24) I. Savatinova, S. Tonchev, E. Popov and L. Mashev: "Electrically induced strip waveguide modes," Opt. Commun. **67**, 4, 261 (1988)
25) E. Popov and L. Tsonev: "Electromagnetic field enhancement in deep metallic gratings," Opt. Commun. **69**, 193 (1989)
26) E. Popov: "Total absorption of light in metallic gratings: a comparative analysis of spectral dependence for shallow and deep grooves," J. Mod. Opt. **36**, 5, 669-674 (1989)
27) L. Mashev, E. Popov and E. Loewen: "Brewster effect for deep metallic gratings," Appl. Opt. **28**, 2538-2541 (1989)
28) E. Popov, L. Mashev and E. Loewen: "Total absorption of light by metallic grating in grazing incidence a connection in the complex plane with other anomalies," Appl. Opt. **28**, 5, 970-975 (1989)
29) L. Mashev and E. Popov: "Anomalies in metallic diffraction gratings," J. Opt. Soc. Am. **6**, 10, 1561-1567 (1989)
30) E. Popov: "Plasmon interactions in metallic gratings: □and k minigaps and their connection with poles and zeros," Surf. Sci. **222**, 517-529 (1989)
31) E. Popov, L. Tsonev, and D. Maystre: "Gratings - general properties in Littrow mount and energy flow distribution," J. Mod. Opt. **37**, 3, 367-377 (1990)
32) E. Popov, L. Tsonev, and D. Maystre: "Losses of plasmon surface wave on metallic grating," J. Mod. Opt. **37**, 3, 379-387 (1990)
33) E. Popov and L. Tsonev: "Total absorption of light by metallic gratings and energy flow distribution," Surf. Sci. **230**, 290-294 (1990)
34) E. Popov, L. Tsonev, E. Loewen and E. Alipieva: "Spectral behavior of anomalies in deep metallic gratings," J. Opt. Soc. Am. A **7**, 1730-1735 (1990)
35) E. Loewen, E. Popov, L. Tsonev and J. Hoose: "Experimental study of local and integral efficiency behavior of a concave holographic diffraction grating," J. Opt. Soc. Am. A **7**, 1764-1769 (1990)

Patents:

E. Popov and L. Mashev: "Method for selective reflectance," Bulgarian patent No 69561
36) L. Mashev, E. Popov, G. Zartov, R. Peeva and K. Panajotov: "Multilayered dielectric diffraction grating," Bulgarian patent No 64731

REFERENCES[1]

1. R.Petit (ed.): in *Electromagnetic Theory of Gratings*, (Springer - Verlag, Berlin, Heidelberg, New York), 1980, ch.1.
1a.R.Petit(ed.): *Electromagnetic Theory of Gratings* (Springer - Verlag, Berlin, Heidelberg, New York) 1980.
2. M.C.Hutley: *Diffraction Gratings* (Academic Press, London, New York) 1982.
3. W.Werner: Appl.Opt.16, 2078 (1977).
4. M.Neviere, D.Maystre and W.R.Hunter: J.Opt.Soc.Am.68, 1106 (1978).
5. M.Neviere, P.Vincent and D.Maystre: Appl.Opt.17, 843 (1978).
6. P.Vincent, M.Neviere and D.Maystre: Nucl.Instr.Meth.152, 123 (1978).
7. P.Vincent, M.Neviere and D.Maystre: Appl.Opt.18, 1780 (1979).
8. G.H.Spencer and M.V.R.K.Murty: J.Opt.Soc.Am.52, 672 (1962).
9. А.Борн и Э.Вольф: Основы оптики, Наука, 1973.
10. E.G.Loewen: *Diffraction Gratings, Ruled and Holographic*, in Appl.Opt. and Opt.Eng., vol.IX, ch.2.
11. P.Vincent and M.Neviere: Opt.Acta 26, 889 (1979).
12. R.Petit and D.Maystre: Rev.Phys.Appl.7, 427 (1972).
13. D.Maystre and R.Petit: J.Spectr.Soc.Jpn.23, suppl., 61 (1974).
14. R.W.Wood: Phil.Mag.4, 396-402 (1902).
15. V.Twersky: IRE Trans. Antennas Propagat. AP-4, 330-345 (1956).
16. V.Twersky: J.Res.Nat.Bur.Stand.64D, 715-730 (1960).
17. R.F.Millar: Can.J.Phys.39, 81-103 (1961).
18. R.F.Millar: Can.J.Phys.39, 104-118 (1961).
19. M.Neviere: "The homogeneous problem", ch.5 of *Electromagnetic Theory of Gratings*, ed. Petit (Springer-Verlag, Berlin, Heidelberg, New York), 1980.
20. D.Maystre: "General study of grating anomalies from electromagnetic surface modes", ch.17 of *Electromagnetic Surface Modes*, ed. Boardman (Wiley, New York), 1982.
21. Lord Rayleigh: Proc.Roy.Soc.(London) A79, 399 (1907).
22. Lord Rayleigh: Phil.Mag.6th ser.14, 60-65 (1907).
23. R.W.Wood: Phis.Rev 48, 928-936 (1935).
24. C.H.Palmer Jr.: J.Opt.Soc.Am.42, 269-276 (1952).
25. J.E.Stewart and W.S.Gallaway: Appl.Opt.1, 421-429 (1962).
26. A.E.Siegman and P.M.Fauchet: IEEE J.Quant.Electron. QE-22, 8, 1384-1402 (1986).
27. U.Fano: J.Opt.Soc.Am.31, 213-221 (1941).
28. A.Hessel and A.A.Oliner: Appl.Opt.4, 1275-1297 (1965).
29. A.Hessel and A.A.Oliner: Opt.Commun.59, 327-330 (1986).
30. D.Y.Tseng, A.Hessel and A.A.Oliner: U.R.S.I. Symposium on Electromagnetic Waves, Alta Freq. 38 special issue, p.82-88 (1969).
31. A.Wirgin and R.Deleuil: J.Opt.Soc.Am.59, 1348-1357 (1969).
32. H.A.Kalhor and A.R.Neureuther: J.Opt.Soc.Am.63, 1412 (1973).
33. A.Hessel, J.Schmoys and D.Y.Tseng:J.Opt.Soc.Am.65,380-384 (1975).
34. J.L.Roumiguieres, D.Maystre and R.Petit: J.Opt.Soc.Am.66, 8, 772-775 (1976).
35. D.Maystre, M.Cadilhac and J.Chandezon: Opt.Acta 28, 457 (1981).
36. D.Maystre and M.Cadilhac: Radio Sci.16, 6, 1003-1008 (1981).
37. M.Breidne and D.Maystre: Proc. SPIE Periodic Structures,

[1] Remark: This is a list of all the refernces cited in the thesis, but not only in the summary.

Gratings, Moire Patterns and Diffraction Phenomena vol.240, 165, (1980).
38. D.Maystre and R.Petit: Opt.Commun.17, 196-200 (1976).
39. M.C.Hutley and D.Maystre: Opt.Commun.19 431 (1976).
40. A.A.Maradudin and A.Wirgin: Surf.Sci.162, 980-984 (1985).
40a. A.Wirgin and A.A.Maradudin: Progress Surf.Sci.22, 1, 1-99 (1986).
41. A.A.Maradudin: Proc.ISCMP(Varna'80, Bulgaria), 1, 11-399 (1981).
42. T.Tamir (ed.): Integrated Optics (Springer, Berlin), 1975.
43. A.W.Snyder and J.D.Love: *Optical Waveguide Theory* (Chapman and Hall, London), 1983.
44. H.Kogelnik: in *Integrated Optics*, Springer, 1975, ed.T.Tamir, ch.2.
45. D.Marcuse: *Theory of Dielectric Optical Waveguides* (Academic, New York), 1975.
46. E.Popov and L.Mashev: Opt.Commun.59, 323 (1986).
47. A.Yariv: IEEE J.Quant.Electron.QE-9, 919 (1973).
48. E.Popov and L.Mashev: J.Opt.Commun.7, 127 (1986).
49. E.Popov and L.Mashev: Opt.Commun.61, 176 (1987).
50. D.Maystre: in *Progress in Optics XXI*, ed.E.Wolf, Elsevier, 1984, ch.1.
51. R.Petit: Rev.Opt.42, 263 (1963).
52. R.Petit: Rev.Opt.45, 249 (1966).
53. W.C.Meecham: J.Appl.Phys.27, 361 (1956).
54. H.Ikino and K.Yasuura: IEEE Trans.Antennas Propag.AP-21, 657 (1973).
55. R.F.Millar: Radio Sci.8, 785 (1973).
56. H.Ikino and K.Yasuura: IEEE Trans.Antennas Propag.AP-24, 884 (1976).
57. M.Cadilhac: in *Electromagnetic Theory of Gratings*, Springer, 1980, ed.R.Petit, ch.2.
58. J.P.Hugonin, R.Petit and M.Cadilhac: J.Opt.Soc.Am.71, 5, 593 (1981).
59. R.Petit and M.Cadilhac: C.R.Acad.Sci.262, 468 (1966).
60. R.F.Millar: Proc.Cambridge Philos.Soc.69, 175 (1971).
61. R.F.Millar: Proc.Cambridge Philos.Soc.69, 217 (1971).
62. M.Neviere and M.Cadilhac: Opt.Commun.2, 235 (1970).
63. P.M.Van den Berg and J.T.Fokkema: J.Opt.Soc.Am.69, 27 (1979).
64. A.Wirgin: C.R.Acad.Sci.B288, 179 (1979).
65. A.Wirgin: C.R.Acad.Sci.B289, 273 (1979).
66. A.Wirgin: C.R.Acad.Sci.A289, 259 (1979).
67. A.Wirgin: Opt.Acta 27, 1671 (1980).
68. A.Wirgin: Opt.Acta 28, 1377 (1981).
69. D.Agassi and T.George: Phys.Rev.B33, 2393 (1986).
70. P.M.Van den Berg: J.Opt.Soc Am.71, 1224 (1981).
71. R.Petit and M.Cadilhac: C.R.Acad.Sci.259, 2077 (1964).
72. A.Wirgin: Rev.Opt.9, 499 (1964).
73. J.L.Uretsky: Ann.Phys.33, 400 (1965).
74. J.Pavageau, R.Eido and H.Kobeisse: C.R.Acad.Sci.264, 424 (1967).
75. A.Wirgin: Rev.Cethedec 5, 131 (1968).
76. A.Neureuther and K.Zaki: Alta Freq.38, 282 (1969).
77. P.M.Van den Berg: Appl.Sci.Res.24, 261 (1971).
78. G.Dumery and P.Filippi: C.R.Acad.Sci.270, 137 (1970).
79. D.Maystre: in *Electromagnetic Theory of Gratings*, Springer, 1980, ed.R.Petit, ch.3.
80. D.Maystre: Opt.Commun.6, 50 (1972).
81. D.Maystre: Opt.Commun.8, 216 (1973).
82. D.Maystre: J.Opt.Soc.Am.68, 490 (1978).

83. D.Maystre: Opt.Commun.26, 127 (1978).
84. L.C.Botten: Opt.Acta 25, 481 (1978).
85. L.C.Botten: J.Opt.11, 161 (1980).
86. P.Vincent: in *Electromagnetic Theory of Gratings*, Springer, 1980, ed.R.Petit, ch.4.
87. M.K.Moaveni, H.A.Kalhor and A.Afrashten: Comput.and Electr.Eng.2, 265 (1975).
88. R.Petit: Rev.Opt.45, 353 (1966).
89. M.Neviere, P.Vincent and R.Petit: Nouv.Rev.Opt.5, 65 (1974).
90. K.C.Chang.V.Shan and T.Tamir: J.Opt.Soc.Am.70, 804 (1980).
91. M.G.Moharam and T.K.Gaylord: J.Opt.Soc.Am.72, 1982).
92. T.K.Gaylord and M.G.Moharam: Proc.IEEE 73, 894 (1985).
93. M.Neviere, G.Cerutti-Maori and M.Cadilhac: Opt.Commun.3, 48 (1971).
94. J.Chandezon, D.Maystre and G.Raoult: J.Opt.11, 235 (1980).
95. J.Chandezon, M.Dupuis, G.Cornet and D.Maystre: J.Opt.Soc.Am.72, 839 (1981).
96. E.Popov and L.Mashev: J.Optics 17, 175 (1986)
97. W.S.Dorn and McCracken: *Numerical Metods with FORTRAN VI case studies*, Wiley, New York, 1972.
98. B.N.Parlett: *The Symmetric Eigenvalue Problem*, Prentice-Hall, 1980.
99. E.Popov and L.Mashev: Opt.Acta 33, 593 (1986).
100. E.Popov and L.Mashev: J.Mod.Opt.34, 155 (1987).
101. K.Wagatsuma, H.Sakaki and S.Saito: IEEE J.Quant.Electr.QE-15, 632 (1979).
102. A.W.Snyder: J.Opt.Soc.Am.62, 1267 (1972).
103. K.K.Swidzinskij: Kwant.Elektr.7, 1914 (1980).
104. D.Maystre and M.Neviere: J.Optics 8, 165 (1977).
105. S.T.Peng, T.Tamir, H.L.Bertoni: IEEE Trans.MTT, MTT-23, 123 (1975).
106. D.G.Hall: Opt.Lett.5, 315 (1980).
107. S.T.Peng and A.A.Oliner: IEEE Trans.MTT, MTT-29, 843 (1981).
108. S.T.Peng and A.A.Oliner: IEEE Trans.MTT, MTT-29, 855 (1981).
109. E.Popov and L.Mashev: Opt.Acta 32, 265 (1985).
110. E.Popov and L.Mashev: Opt.Acta 32, 635 (1985).
111. E.Popov and L.Mashev: Opt.Commun.52, 393 (1985).
112. A.Yariv and M.Nakamura: IEEE J.Quant.Electr.QE-13, 233 (1977).
113. K.Yasumoto and M.Murayama: Technical Report CSCE-86-A02, Fukuoka, Japan (1986).
114. G.I.Stegeman, D.Sarid, J.J.Burke and D.G.Hall: J.Opt.Soc.Am.71, 1497 (1981).
115. E.Popov, L.Tsonev, and D.Maystre: J.Mod.Opt.37, 379 (1990).
116. E.Popov, L.Tsonev, and D.Maystre: J.Mod.Opt.37, 367 (1990).
117. J.V.Hajnal: Proc.R.Soc.Lond.A414, 447-468 (1987).
118. E.Popov, L.Mashev and D.Maystre: Opt.Acta 33, 607 (1986).
119. J.R.Andrewartha, J.R.Fox and I.J.Wilson: Opt.Acta 26, 1, 69-89 (1979).
120. J.R.Andrewartha, J.R.Fox and I.J.Wilson: Opt.Acta 26, 2, 197-209 (1979).
121. E.Popov, L.Mashev and E.Loewen: Appl.Opt.28, 970 (1989).
122. D.Maystre and M.Neviere: J.Opt.8, 165 (1977).
123. D.Maystre, M.Neviere, R.Reinisch and J.L.Coutaz: J.Opt.Soc. Amer.B5 338 (1988).
124. M.Neviere and R.Reinish: J.Phys.(Paris) 44, suppl.12, C10-359 (1983).
125. R.Reinisch, G.Chartier, M.Neviere, M.C.Hutley, G.Clauss,

J.P.Galaup and J.F.Eloy, J.de Physique-Lett.44 L1007 (1983).
126. J.L.Coutaz: J.Opt.Soc.Amer.B4, 105 (1987).
127. M.Neviere, H.Akhouayri, P.Vincent and R.Reinisch: Proc. Soc. Photo-Opt. Instrum. Eng. 815, 146 (1987).
128. J.L.Coutaz and R.Reinisch: Solid St.Commun.56, 545 (1985).
129. K.Metcalfe and R.Hester: Chem.Phys.Lett.94, 411 (1983).
130. M.Yamashita and M.Tsuji: J.Phys.Soc.Jap.52 2462 (1983).
131. R.Renisch and M. Neviere: Opt.Engng.20, 629 (1981).
132. L.Mashev, E.Popov and E.Loewen: Appl.Opt.28, 2538-2541 (1989).
133. E.Popov and L.Tsonev: Surf.Sci., to be published.
134. E.Popov and L.Tsonev: Opt.Commun.69, 193 (1989).
135. L.Mashev: *Relief holographic diffraction gratings*, PhD thesis, Sofia, 1985.
136. L.Mashev and S.Tonchev: Appl.Phys.A26, 143 (1981).
137. L.Mashev and E.Popov: J.Opt.18, 3 (1987).
138. B.Racz, Zs.Bor, S.Szatmari and G.Szabo: Opt.Commun.366, 399 (1981).
139. L.B.Mashev, E.K.Popov and E.G.Loewen: Appl.Opt.26, 4738 (1987).
140. L.Mashev, E.Popov and E.Loewen: Appl.Opt.27, 152 (1988).
141. L.Mashev, E.Popov and D.Maystre: Opt.Commun.67, 321 (1988).
142. E.Popov, L.Tsonev, E.Loewen, and E.Alipieva: J.Opt.Soc.Am., to be published.
143. F.Toigo, A.Marvin, V.Celli and N.R.Hills: Phys.Rev.B15, 5618 (1977).
144. N.E.Glass, H.G.Weber and D.L.Hills: Phys.Rev.B29, 6548 (1984).
145. D.Heitmann, N.Kroo, Ch.Schulz and Zs.Szentirmay: Phys.Rev.B35, 2660 (1987).
146. H.Jonsson, J.H.Weare, T.H.Ellis and G.Scoles: Surf.Sci.180, 353 (1987).
147. P.Tran, V.Celli and A.A.Maradudin: Opt.Lett.13, 530 (1988).
148. E.Popov: Surf.Sci.222, 517 (1989).
149. I.A.Avrutskii, G.A.Golubenko, V.A.Sychugov, and A.V.Tischenko: Kwant.Elektr.13, 1629 (1986).
150. E.Popov: J.Mod.Opt.36, 669 (1989).
151. L.Mashev and E.Popov: J.Opt.Soc.Am.6, 10, 1561-1567 (1989).
152. L.Mashev and E.Popov: Opt.Commun.55, 377 (1985).
153. G.Haas and R.E.Thun (eds.): *Physics of Thin Films*, Advances in Research and Development, vol.2, ch.6, (Academic Press, New York and London), 1964.
154. L.Mashev and E.Popov: Opt.Commun.51, 131 (1984).
155. G.A.Golubenko, A.S.Svakhin, V.A.Sychugov, A.V.Tischenko, E.Popov and L.Mashev: J.Opt.Quant.Electr.18, 123 (1986).
156. E.Popov, L.Mashev and D.Maystre: Opt.Commun.65, 97 (1988).
157. E.Popov and L.Tsonev: unpublished.
158. R.C.Enger and S.K.Case: J.Opt.Soc.Am.73, 1113 (1983).
159. K.Yokomori: Appl.Opt.23, 2303 (1984).
160. P.Yeh: *Optical waves in layered media*, Wiley series in Pure and Applied Optics (Wiley, New York), 1988.
161. I.A.Avrutskii, V.P.Duraev, E.T.Nedelin, A.M.Prohorov, A.S.Svakhin, V.A.Sychugov and V.A.Tisschenko: Kwant.Elektr.15, 569 (1988).
162. W.A.Sychugow, A.W.Tishchenko i A.A.Hakimow: Pisma JTF 5, 937 (1979).
163. L.Mashev, S.Tonchev and E.Popov: Bulg.J.Phys.12, 297 (1985).
164. G.Korn and T.Korn: *Mathematical Handbook* (McGraw-Hill Book Co, New York), 1968.